

ATMOSPHERIC TRACER STUDIES TO CHARACTERIZE THE TRANSPORT  
AND DISPERSION OF POLLUTANTS IN THE CALIFORNIA DELTA REGION

VOLUME I  
PRESENTATION AND DISCUSSION OF RESULTS

Contract No. ARB-A5-065-87

June 15, 1977

Prepared for:

State of California  
Air Resources Board  
1709 11<sup>th</sup> Street  
Sacramento, California 95814

by

Brian K. Lamb

and

Fredrick H. Shair  
(Principal Investigator)

Division of Chemistry and Chemical Engineering  
California Institute of Technology  
Pasadena, California 91125

The statements and conclusions in this report are those of the contractor and not necessarily those of the California Air Resources Board. The mention of commercial products, their source or their use in connection with material reported herein is not to be construed as either an actual or implied endorsement of such products.

LIBRARY  
AIR RESOURCES BOARD  
P. O. BOX 2815  
SACRAMENTO, CA 95812

## SUMMARY

Eight atmospheric tracer studies, utilizing  $\text{CBrF}_3$  and/or  $\text{SF}_6$ , were conducted from August 31, 1976, through September 14, 1976, within the California Delta Region during four designated meteorological periods. The purpose of these tests was to quantitatively determine the transport and dispersion characteristics of the air passing over the Montezuma Hills. The data base was comprehensive enough to permit accurate mass balances of the tracer; essentially all of the tracer was accounted for by this analysis. Due to the steadiness of the winds, the plume trajectories at 10 km and 50 km downwind of the Montezuma Hills were found to be quite similar. On the average, plumes emitted from the Montezuma Hills during the test periods were transported southeast over Stockton. As a result of the steady nature of the winds, the commonly used Hino correction was found to grossly underestimate the hourly-averaged tracer concentrations computed from 10-second averaged concentrations. A comparison of experimentally determined dispersion parameters with those associated with Pasquill atmospheric stability classes indicated that atmospheric stability generally decreases with increasing distance downwind from the Montezuma Hills. In spite of the complex meteorology and terrain, estimates of tracer concentrations based upon the Gaussian plume model were found to be reasonably accurate. A nomograph was developed to permit rapid calculation of non-reactive pollutant concentrations from tracer data and pollutant emission rates; in the case of  $\text{NO}_2$ , the oxidation of  $\text{NO}$  to  $\text{NO}_2$  was assumed to be rapid relative to the transport time. The nomograph was used to predict ground level concentrations of pollutants resulting from the projected emissions associated with the proposed Dow complex in the Montezuma Hills. A reasonable correlation was found to exist between the horizontal standard deviation of the wind,  $\sigma_\theta$ , and the horizontal dispersion parameter of the plume,  $\sigma_y$ . Air parcel trajectories, based upon Goodin's (1977) numerical solution to the two-dimensional mass balance equation were found to be in excellent agreement with the tracer data. The correlation between  $\sigma_\theta$  and  $\sigma_y$ , along with the trajectory analysis provide a means for extending the results of this study to other periods of the year. This investigation indicates where emissions from the Montezuma Hills should be monitored. Finally, these results suggest that further study regarding the chemistry, transport and dispersion of pollutants entering the San Joaquin Valley will be of considerable interest.

## ACKNOWLEDGMENT

We are very happy to acknowledge Charles L. Bennett and Jack K. Suder, both Senior Air Pollution Research Specialists with the California Air Resources Board, for their interest, helpful suggestions, and their help in coordinating this program.

The cooperation of William Anderson and David Bauer of the Dow Chemical Company was greatly appreciated. We wish to thank Art Schafer and L. Willard Richards of Rockwell International for their support.

We wish to thank John Pryshepa of Caltrans for the use of their portable anemometers. We thank Norman Baker for his support in providing airborne sampling and pertinent meteorological data. We thank Neal Moyer of the Air Resources Board for providing emission data, and Burton Okin of the Bay Area APCD for providing meteorological data.

Personnel from Meteorology Research, Incorporated provided meteorological support and also collected airborne samples. In particular, we wish to thank Ted B. Smith, Hans D. Giroux, and William Knuth for their cooperation throughout the field study.

We thank Joseph Spano of the San Joaquin APCD for his support in providing air sampling sites. We also thank the California State Police along with local firefighters for providing a number of air sampling sites. The Pinole police department was very cooperative in providing a release location. We express our thanks to the many people at APCD stations, private businesses, and homes who allowed us to operate the hourly air sampling systems.

We wish to thank C. Ray Dickson of the NOAA Laboratories in Idaho Falls, Idaho, for helpful suggestions regarding the development of chromatographic columns which were used to separate  $\text{SF}_6$  and  $\text{CBrF}_3$ .

We thank Russell Bennett and Dave Suder for their help in obtaining air samples during the field study.

We wish to thank George Griffith, Henry Smith, Ray Reed, and John Yehle for their willingness to lend a hand when the need arose. We also thank Sharon ViGario for her patience in the typing of this report.

Finally, we thank the management of the California Holiday Lodge for permitting us to set up a small laboratory on their premises.

## PERSONNEL

The following persons participated in the 1976 California Delta tracer field studies:

1. Mr. Bart Croes
2. Mr. Andrew Falls
3. Mr. Arthur Gooding
4. Mr. Jim Hickey
5. Mr. Eric Kaler
6. Mr. Brian Lamb
7. Mrs. Margaret Lamb
8. Mr. Wing Hong Lee
9. Mr. Ernest Sasaki
10. Dr. Fredrick Shair
11. Mr. Peter Shair
12. Mr. Jim Westover

## TABLE OF CONTENTS

Volume I

	<u>Page</u>
Summary: Volume I	iii
Acknowledgment	iv
Personnel	v
Table of Contents: Volume I	vi
Table of Contents: Volume II, Parts A and B	viii
List of Tables	x
List of Figures	xi
1. Introduction	1
1.1 Industrialization of the California Delta Region	1
1.2 Literature Review	4
1.3 Objectives of the California Delta Tracer Study	7
2. Meteorology and Topography of the California Delta Region	8
3. Experimental Procedure	15
3.1 Field Test Design and Schedule	15
3.2 Tracer Release System	15
3.3 Air Sampling Systems	17
3.31 Automobile Traverse System	17
3.32 Airborne Air Sampling System	17
3.33 Hourly Average Sequential Samples	17
3.4 Chemical Analysis of Air Samples	27
3.5 Meteorological Support Systems	33
3.51 Surface Wind Data	33
3.52 Upper Air Wind Data	33
4. Presentation and Discussion of Results	39
4.1 Relation of Tracer Data to Industrial Pollutant Emissions	39
4.2 Description of the Tracer Tests	48

Table of Contents, Volume I (Continued)

	<u>Page</u>
4.21 Tracer Test 1 (8/31/76)	48
4.22 Tracer Test 2 (9/2/76)	54
4.23 Tracer Test 3 (9/5/76)	67
4.24 Tracer Test 4 (9/6/76)	76
4.25 Tracer Test 5 (9/9/76)	86
4.26 Tracer Test 6 (9/10/76)	91
4.27 Tracer Test 7 (9/13/76)	102
4.28 Tracer Test 8 (9/14/76)	116
4.3 Determination of Dispersion Parameters: from Auto- mobile Traverse and Airborne Spiral Tracer Data	122
4.4 Mass Balance of Tracer Data	134
4.5 Analysis of Dispersion	142
4.6 Use of Field Study Data for Air Quality Model Development	182
4.7 Applicability of the Gaussian Plume Model in the California Delta Region	182
4.8 Relation of Dispersion Data to Fluctuations of the Wind	210
4.9 Estimated Maximum Pollutant Concentrations	230
5. Calculation of the Surface Wind Field	236
Appendix A (Gas Chromatograph Calibration Results)	258
Appendix B (Calculation of Plume Parameters from Crosswind Traverses)	260
Literature Cited	264

TABLE OF CONTENTS  
VOLUME II, PARTS A AND B

<u>Part A</u>	<u>Page</u>
Summary: Volume II, Parts A and B	iii
Acknowledgment	v
Personnel	vi
Table of Contents	vii
List of Tables	ix
List of Figures	x
1. Introduction	1
2. Experimental Procedure	4
3. Presentation of Tracer Data	21
3.1 Relation of Tracer Data to Industrial Pollutant Emissions	21
3.2 Overview of Tracer Data	25
3.3 Automobile Traverse Tracer Data	93
3.4 Airborne Traverse Tracer Data	122
3.5 Airborne Spiral Tracer Data	130
3.6 Automobile Traverse Best-fit Gaussian Curves	133
3.7 Airborne Spiral Best-fit Gaussian Curves	165
3.8 Hourly Averaged Tracer Data	168
3.9 Hourly Averaged Crosswind Tracer Concentrations	183
3.10 Mass Balance of Tracer Data	187
3.11 Crosswind Horizontal and Vertical Standard Deviations as Functions of Downwind Distance	193
3.12 Comparison of Experimental Dispersion Results with Pasquill Dispersion Parameters	228
4. Relationship of Dispersion Data to Wind Data	257
4.1 Fluctuations in the Horizontal Winds	257
4.2 Horizontal Dispersion as a Function of Wind Fluctuations	260
4.3 Atmospheric Stability Classification	262



## LIST OF TABLES

	<u>Page</u>
1. Daily Average Wind Summary for the Dow and Brentwood Stations.	12
2. Tracer Release Data.	16
3. Descriptions of Automobile and Airborne Traverses and Airborne Spirals.	18
4. Location of Hourly Averaged Sequential Air Samplers.	28
5. Wind Data Stations and Description of Wind Data.	34
6. Projected Dow Emissions and Associated Nomograph K Values.	43
7. Pollutant Emissions from Major Point Sources in the Northeastern Bay Area.	45
8. Average Meteorological Conditions During the Field Tests.	49
9. Best-fit Gaussian Curve Results.	129
10. Tracer Mass Balance Results.	138
11. Horizontal and Vertical Crosswind Dispersion Coefficients.	147
12. Stack Characteristics from the Dow Montezuma Hills Plant.	205
13. Comparison of 10-second and Hourly Averaged Maximum Tracer Concentrations.	220
14. Maximum Pollutant Concentrations Due to Projected Dow Emissions.	231
15. Comparison of NO <sub>2</sub> Concentration Measurements and Estimations.	234
A-1 Gas Chromatograph Calibration Results.	258
A-2 Gas Chromatograph Cross-Check Results.	259

## LIST OF FIGURES

	<u>Page</u>
1. The California Delta Region.	3
2. Prevailing west and northwest wind flow types.	9
3. Topographical map of the Bay Area, California Delta, and San Joaquin Valley.	13
4. Typical tracer chromatogram.	30
5. Gas chromatograph calibration curves for dual tracers.	32
6. Location of surface wind and upper air data stations.	38
7. Conversion nomograph for converting SF <sub>6</sub> tracer concentrations to pollutant concentrations.	41
8. Conversion nomograph for converting CBrF <sub>3</sub> tracer concentrations to pollutant concentrations.	42
9. Surface wind streamlines, 1600 PDT, 8/31/76.	50
10. Overview of automobile traverse tracer data, Test 1.	52
11. Hourly averaged crosswind SF <sub>6</sub> profiles measured along Highway 160, Test 1.	53
12. Hourly averaged crosswind SF <sub>6</sub> profiles measured along Highway 99, Test 1.	55
13. Overview of hourly averaged SF <sub>6</sub> data, Test 1.	56
14. Surface wind streamlines, 1600 PDT, 9/2/76.	57.
15-17. Overview of automobile traverse tracer data, Test 2.	59-61
18. Hourly averaged crosswind CBrF <sub>3</sub> profiles measured along Highway 160, Test 2.	62
19. Hourly averaged crosswind SF <sub>6</sub> profiles measured along Highway 160, Test 2.	64
20. Overview of hourly averaged SF <sub>6</sub> data, Test 2.	65
21. Hourly averaged crosswind SF <sub>6</sub> profiles measured along Highway 99, Test 2.	66
22. Surface wind streamlines, 0100 PDT, 9/5/76.	68

## List of Figures (Continued)

	<u>Page</u>
23-24. Overview of automobile traverse SF <sub>6</sub> data, Test 3.	69-70
25. Overview of hourly averaged SF <sub>6</sub> data, Test 3.	72
26-28. Hourly averaged crosswind SF <sub>6</sub> profiles measured along Highway 99, Test 3.	73-75
29. Surface wind streamlines, 1900 PDT, 9/6/76.	77
30-31. Overview of automobile traverse SF <sub>6</sub> data, Test 4.	78-79
32. Overview of hourly averaged SF <sub>6</sub> data, Test 4.	81
33-36. Hourly averaged crosswind SF <sub>6</sub> profiles, measured along Highway 99.	82-85
37. Surface wind streamlines, 1300 PDT, 9/9/76.	88
38-39. Overview of automobile traverse SF <sub>6</sub> data, Test 5.	89-90
40. Surface wind streamlines, 1000 PDT, 9/10/76.	92
41-42. Overview of automobile traverse SF <sub>6</sub> data, Test 6.	93-94
43,45-46. Overview of airborne traverse SF <sub>6</sub> data, Test 6	95, 98-99
44. Vertical SF <sub>6</sub> profile observed over Frank's Tract Recreation Area, Test 6.	97
47. Overview of hourly averaged SF <sub>6</sub> data, Test 6.	100
48. Hourly averaged crosswind SF <sub>6</sub> profiles, Test 6.	101
49. Surface wind streamlines, 1000 PDT, 9/13/76	103
50-54. Overview of automobile traverse tracer data, Test 7.	104-108
55,57-58. Overview of airborne traverse tracer data, Test 7.	111, 113-114
56. Vertical SF <sub>6</sub> profiles observed 0.8 Km north of the Port Chicago Naval Depot.	112
59. Overview of hourly averaged SF <sub>6</sub> data, Test 7.	115
60. Surface wind streamlines, 1000 PDT, 9/14/76	117

## List of Figures (Continued)

	<u>Page</u>
61-62. Overview of automobile traverse SF <sub>6</sub> data, Test 8.	118- 119
63. Overview of airborne traverse SF <sub>6</sub> data, Test 8.	120
64. Vertical SF <sub>6</sub> profile observed 0.8 Km north of the Port Chicago Naval Depot.	121
65-66. Typical best-fit Gaussian curves to automobile traverse tracer data.	125- 126
67-68. Best-fit Gaussian curves to airborne spiral tracer data.	127- 128
69. Horizontal crosswind dispersion parameter, $\sigma_y$ , as a function of distance downwind of the Dow site.	143
70. Vertical crosswind dispersion parameter, $\sigma_z$ , as a function of distance downwind of the Dow site.	144
71. Vertical crosswind dispersion parameter, $\sigma_z$ , as a function of distance downwind of the Pinole site.	145
72. Vertical crosswind dispersion parameter, $\sigma_z$ , as a function of distance downwind of the Pinole site.	146
73-78. Horizontal and vertical crosswind dispersion parameters, $\sigma_y$ and $\sigma_z$ , as functions of downwind distance (by meteorological period).	152- 157
79-92. Comparison of horizontal and vertical dispersion of tracer plumes with the dispersion of plumes associated with Pasquill atmospheric stability classes (by test).	158- 171
93. Horizontal crosswind dispersion parameter, $\sigma_y$ , as a function of distance downwind of the Dow site compared with the dispersion parameter associated with Pasquill atmospheric stability classes (by meteorological period).	175
94. Vertical crosswind dispersion parameter, $\sigma_z$ , as a function of distance downwind of the Dow site compared with the dispersion parameter associated with Pasquill atmospheric stability classes (by meteorological period).	176
95. Horizontal crosswind dispersion parameter, $\sigma_y$ , as a function of distance downwind for tracer releases from Pinole and Martinez and the dispersion parameter associated with Pasquill atmospheric stability classes (by meteorological period).	177

## List of Figures (Continued)

	<u>Page</u>
96. Vertical crosswind dispersion parameter, $\sigma_z$ , as a function of distance downwind for tracer releases from Pinole and Martinez, and the dispersion parameter associated with Pasquill atmospheric stability classes (by meteorological period).	178
97-108. Centerline tracer concentrations compared with centerline concentrations predicted using the Gaussian plume model.	185-197
110-112. Crosswind tracer profiles compared with crosswind profiles predicted using the Gaussian plume model.	201-203
113-115. Centerline tracer concentrations compared with centerline concentrations predicted using the Briggs plume rise model and the Gaussian plume model.	207-209
116-117. Horizontal standard deviation of the wind as a function of time of day.	211-212
118. Plume centerline concentration as a function of distance north of the Highway 4 - Highway 160 junction along Highway 160.	214
119. Plume centerline concentration as a function of distance south of Sacramento along Highway 99	215
120. Average plume centerline positions for plumes emitted from the Dow site in the Montezuma Hills.	216
121. Horizontal crosswind standard deviation, $\sigma_y$ , as a function of the horizontal standard deviation of the wind, $\sigma_\theta$ .	222
122. Horizontal standard deviation of the wind, $\sigma_\theta$ , as a function of time of day for different averaging periods.	225
123-125. Horizontal crosswind standard deviation, $\sigma_y$ , as a function of the horizontal standard deviation of the wind, $\sigma_\theta$ , for different averaging times.	226-228
126. Estimation of distance downwind of the Montezuma Hills where the concentration of $\text{NO}_2$ (caused by projected Dow emissions) equals maximum ambient levels.	233
127. California Delta Region wind calculation grid system.	237

## List of Figures (Continued)

		<u>Page</u>
128- 139	Hourly surface wind vectors, 1200-2300 PDT, 8/31/76.	239- 250
140- 142.	Hourly upper air wind vectors, 1700 PDT, 8/31/76.	251- 253
143.	Forward air parcel surface trajectories from the Montezuma Hills, 8/31/76.	255
144.	Forward air parcel surface trajectories from Pinole and Martinez, 8/31/76.	257

## 1. Introduction

### 1.1 Industrialization of the California Delta Region

Interbasin air flow between the Bay Area of San Francisco and the Sacramento and San Joaquin Valleys of central California is characterized during the summer months by a sharp low-level temperature inversion (Miller, 1968) and a strong diurnal sea breeze (Fosberg and Schroeder, 1966). A northern component of the marine air flows through the Bay Area, channels into the Carquinez Strait and fans across the Delta region of the Sacramento and San Joaquin Rivers (Smalley, 1957). Ultimately, the air passing over the heavily populated and industrialized Bay Area passes from the Delta region into the Sacramento and San Joaquin Valleys. The presence of large industrial complexes, projected for construction in the Montezuma Hills of the Delta region, may add to the levels of atmospheric pollutants already present in the air passing through the area. The existence of the urban centers upwind and downwind of the proposed construction sites, the rugged terrain surrounding the Bay Area, and the complex meteorological patterns in the region prohibit simple predictions of the impact associated with future industrialization. An analysis of the extent of adverse impact upon air quality which may result from industrial development of the Montezuma Hills requires a study of the transport and dispersion of pollutants emitted within the Delta region and the Bay Area. The use of atmospheric tracer techniques, utilizing gaseous tracers such as  $\text{SF}_6$  and  $\text{CBrF}_3$ , provides a relatively simple and inexpensive means to obtain important data which can be used to assist in the impact analysis. The results from eight full-scale

tracer studies conducted in the California Delta Region (shown in Figure 1) during September, 1976, are presented in this report. The cost of these tracer studies was less than .02% of the capital investments required for the construction of just one of the proposed industrial facilities.



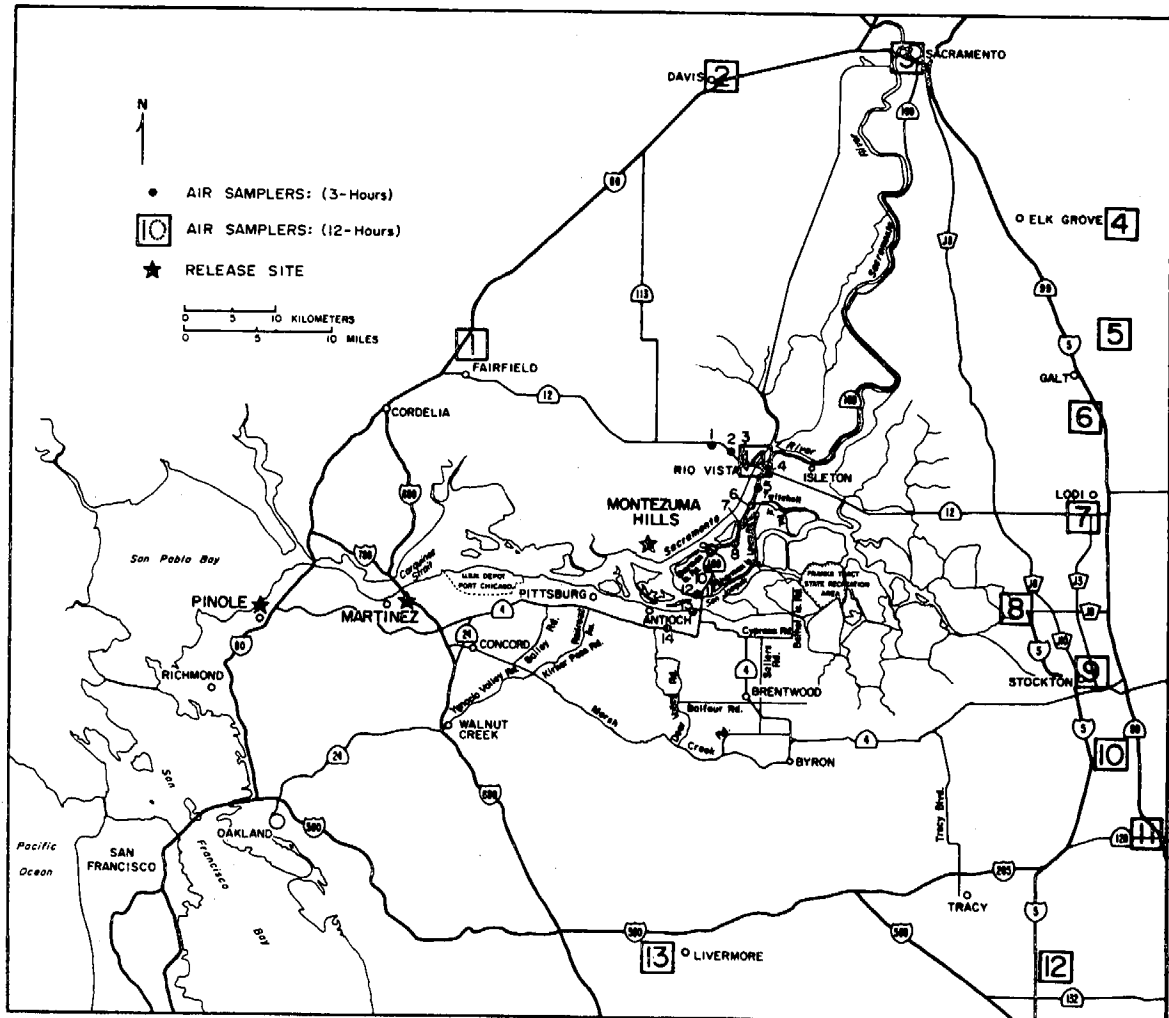


Figure 1. The California Delta Region.

## 1.2 Literature Review

The transport and dispersion of pollutants under complex topographical and meteorological conditions have been the concern of a growing list of workers (Pasquill, 1974). Start, et al. (1974) used tracer techniques in Utah to determine the amount of dilution which occurs for airborne material passing over and around mountains and canyons. They concluded that enhanced mechanical turbulence associated with rough terrain increased dilution over that found in flat regions. Terrain effects were found to increase with increasing stability. Similar conclusions were reached by Giroux, et al. (1974) from a tracer test conducted in southern California. In that test, the  $\text{SF}_6$  tracer was followed as far as 40 km downwind of the release point. MacReady, et al. (1974) agreed with the preceding reports in suggesting that turbulence was generated from topographical-induced horizontal divergence patterns. From the results of diffusion tests in the Point Arguello area of southern California, Hinds (1970) found that "daytime (unstable) conditions minimized the importance of terrain whereas nighttime (stable) conditions led to apparently significant interactions between terrain and synoptic scale weather events." Angell, et al. (1966,1976) used tetroons to study pollutant trajectories through the southern California air basin. Tetroons released along the coast in some instances were carried out to sea and then, with the diurnal reversal of the winds, swept back into the interior of the basin. In the latter work (1976), tetroons released in early morning near Los Angeles were tracked eastward through the Puente Hills as far as San Bernardino. Other tetroons, released under more

stagnant conditions, moved south before turning east into the Santa Ana Canyon.

Previous work in this laboratory has attempted to characterize the transport and dispersion of pollutants in California coastal areas. Drivas and Shair (1974) released 33.5 Kg of  $\text{SF}_6$  over 45 minutes from Anaheim, California, and followed the tracer through five neighboring communities as far as Palm Springs, 124 km downwind. These authors (1975) also conducted full-scale tracer studies from power plant stacks in both the Moss Landing and Long Beach coastal zones of California. Afternoon tracer plumes from Moss Landing were observed to move southeast through the Salinas Valley. Afternoon tracer plumes from Long Beach were transported northeast toward Fullerton and Pomona, and then eastward toward San Bernardino. Lamb and Shair (1977) conducted a tracer study from the Oxnard Plain in Ventura County and found that plumes were transported east along the coast and along an inland route into the San Fernando Valley of the Los Angeles Air Basin. These studies reflect the usefulness of tracer techniques in studying the transport and dispersion of pollutants under complex coastal meteorological and topographical conditions.

Fosberg, et al. (1976) attempted to account for the effects of mass divergence upon pollutant dispersion by modifying the well-known Gaussian plume model. Inclusion of a divergence term in the Gaussian expression decreased calculated pollutant concentrations by as much as a factor of two. In other work using the Gaussian plume model, Peters and Richards (1977) developed a scheme to incorporate fast reversible

chemical reactions into dispersion models. Application of the procedure to the conversion of NO to NO<sub>2</sub> by reaction with ozone and to the reaction of sulfuric acid with ambient ammonia was presented. This procedure is based on the assumption that local chemical equilibria is achieved at each receptor site. Liu, et al. (1976) showed how to modify the Gaussian dispersion terms to account for the roughness of the terrain. Their derivation of the modified dispersion parameters was based on development of the relationship of the eddy diffusivities and the Gaussian dispersion parameters. Liu, et al. found that for a surface roughness of 50 cm the modified dispersion parameters resulted in a decrease in concentration by a factor of two from the conventional Gaussian model.

Several authors have utilized forms of the diffusion equation to develop dispersion models which take into account the effects of terrain. Roffman and Grimble (1974) developed a three-dimensional model based on successive coordinate transformations where one coordinate was required to be parallel to the flow during each segment of the transport path. Reynolds, et al. (1973) used a coordinate transformation to take into account the irregularity of the floor of the Los Angeles Air Basin.

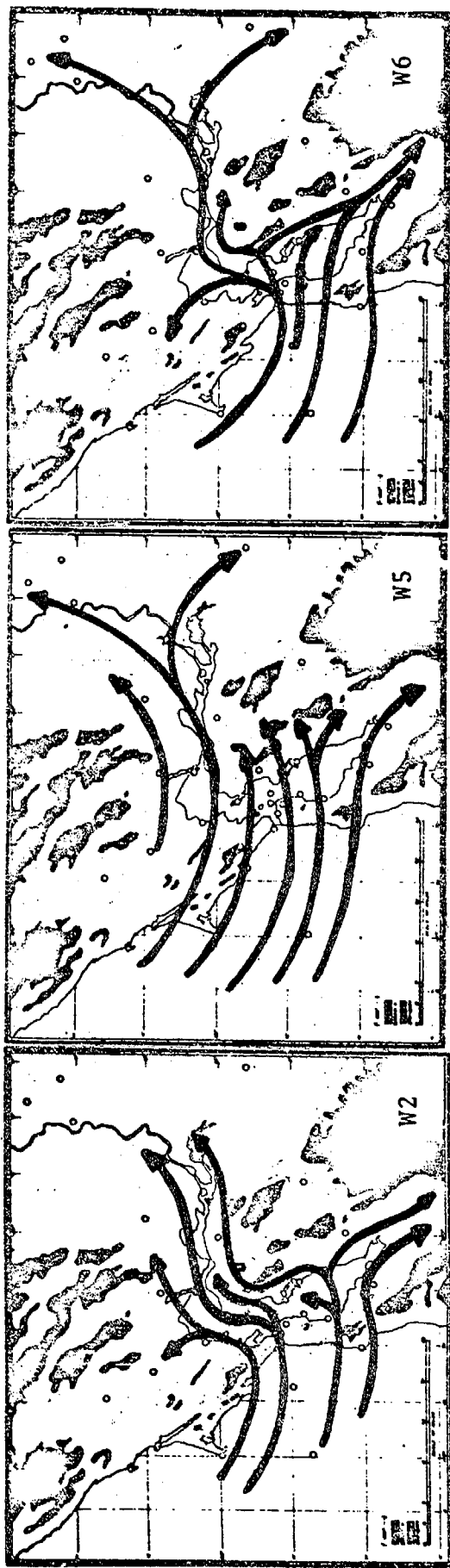
The experimental studies cited above generally indicate that pollutants are dispersed to a greater extent over complex terrain than over flat surfaces. Furthermore, under stable atmospheric conditions, the effects of terrain upon dispersion and transport are increased over that observed under unstable conditions. Transport paths over complex terrain within complicated meteorological patterns appear to be relatively

difficult to predict on a quantitative basis. Efforts are progressing on the modification and development of atmospheric dispersion models to account for the effects of terrain and meteorology upon the transport and dispersion of pollutants.

## 2. Meteorology and Topography of the California Delta Region

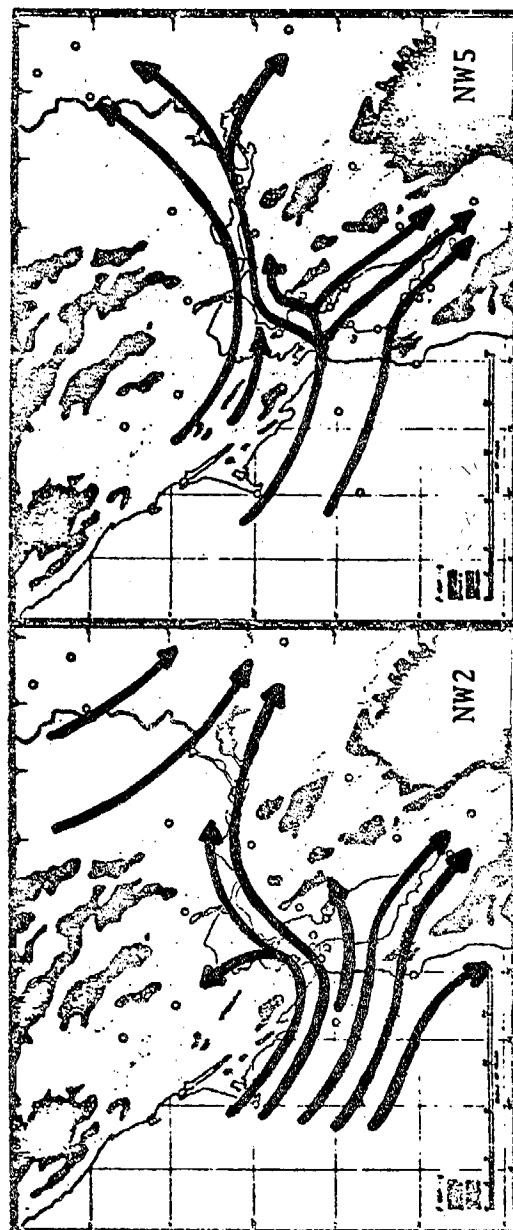
Surface wind patterns from Smalley (1957) indicate that the Carquinez Strait is the major channel for air flow over the Delta Region. During September in the years 1952-1955, the surface wind patterns most prevalent in the area were the west and northwest wind flow types shown in Figure 2. According to Smalley, these patterns occurred 51% of the time, and light and variable winds accounted for 23% of the time. Patterns W5, W2, and W6 were most often observed; they occurred 14%, 10%, and 10% of the time, respectively. These surface patterns show how marine air can become laden with urban pollutants in the Bay Area, pass over the Delta Region, and then turn either north to Sacramento or south to Stockton. Fosberg and Schroeder (1966) explained the onshore summer flow patterns as the result of strong pressure and temperature gradients developed from the coexistence of the eastern Pacific subtropical high pressure area off the coast and a thermal trough in the interior.

Wind flow from the Bay Area through the Delta typically centers around the daily occurrence of an afternoon sea breeze. Fosberg and Schroeder (1966) pointed out that this sea breeze, which is caused by differential heating and cooling of the land and sea, is superimposed upon the summer marine air flow. Miller (1968) noted that the central California sea breeze was accompanied by a sharp, low-level temperature inversion extending inland as far as 40 km. The diurnal cycle can be divided into four periods of the day (Smith, 1976). During Sea Breeze conditions, from approximately 1300 to 1800, winds are relatively strong throughout the area. The average wind speeds at Martinez, Sacramento, and Stockton during the Sea Breeze test periods were respectively, 5 m/sec,



9

Figure 2. Prevailing west and northwest wind flow types, Smalley (1957).



2 m/sec, 4 m/sec. Smalley noted that wind flow types W5 and W6 accounted for 40% of the patterns observed at 1600 hours. In the afternoon, the mixing depth reaches a maximum due to the heating of the land. Typical afternoon mixing depths during the test period were between 1000 and 3000 meters. This pattern is opposite to that which occurs during Nighttime conditions from approximately midnight to 0500. At night, the height of the mixing layer drops to a minimum, typically between 100 and 500 meters. Air flow stagnates as drainage from the Sierra Nevada Mountains meets the weak sea flow over the Central Valley. According to the Smalley report, light and variable winds occurred during 38% of the measurements taken at 0400; west wind types accounted for 39% of measurements in the early morning. Two transition periods separate the Sea Breeze and Nighttime regimes: Pre-Sea Breeze conditions occur from approximately 0600 to 1100 and are characterized by lifting of the nighttime mixing layer and development of the marine air flow. Wind type W2 was observed in 13% of the patterns at 1000, and light and variable winds were measured during 28% of the time at 1000. Sea Breeze Tail conditions follow the afternoon period and are typified by a decrease in mixing height and a decrease in the strength of the coastal flow. West wind flows in the Smalley work existed in 48% of the observations taken at 2200.

As a result of this summertime meteorological cycle, a strong, relatively constant jet of air issues from the Carquinez Strait and fans out into the reaches of the Delta Region and Central Valley. Fosberg and Schroeder (1966) indicated that the wind surge associated with the invading marine air gains speed as it passes through the Carquinez Strait where it combines with the intensely channeled summer



marine flow. It appears that part of this jet maintains its strength past the Montezuma Hills and then dissipates fairly rapidly just beyond the area. For example, during the two-week test period in early September, the average surface wind speed at the Dow site in the Montezuma Hills was 7 m/sec; further downwind, at Brentwood, the average surface wind speed was 2 m/sec. The daily average wind speeds measured at two levels at the Dow site and at the surface at Brentwood are given in Table 1.

The existence of this jet suggests that material emitted from the Montezuma Hills may be carried into the Central Valley within a narrow, stable stream of air. Material emitted west of the Carquinez Strait into the marine flow may be widely dispersed by the divergence of air from the Strait. Pollutants emitted from sources located very near one another in the vicinity of the Carquinez Strait may be transported along widely different trajectories into the Sacramento or San Joaquin Valleys.

Terrain effects on air flow through the Carquinez Strait appear to be very important in determining pollutant trajectories through the Delta Region. In a Bay Area tracer study utilizing fluorescent particles, Sandberg, et al. (1970) found that the hilly terrain surrounding San Francisco Bay served to deflect westerly marine air flow into the northerly and southerly trajectories apparent in the Smalley wind patterns. Sandberg noted that the presence of low-level temperature inversions enhanced the effects of the Bay Area terrain upon air flow. Results from the tracer study showed that the hilly terrain increased pollutant dispersion, but channeling through such terrain caused higher concentrations to occur locally. The map in Figure 3 shows the topographical contour

12  
TABLE 1

DAILY AVERAGE WIND SUMMARY FOR THE DOW AND BRENTWOOD STATIONS

Date	Dow (surface)		Dow (tower)		Brentwood (surface)	
	10 meters		56 meters		10 meters	
	Ave. Speed	Prevailing	Ave. Speed	Prevailing	Ave. Speed	Prevailing
	(m/sec)	Direction	(m/sec)	Direction	(m/sec)	Direction
Aug. 30	5.6	W	7.2	W	2.6	NW
" 31	7.3	W	8.5	W	2.5	N
Sept. 1	9.6	W	10.2	W	2.1	NNE
" 2	8.9	W	9.7	W	2.2	NNE
" 3	9.6	W	10.7	W	2.3	N
" 4	8.9	W	10.2	W	2.3	NNE
" 5	8.5	W	9.6	W	2.3	N
" 6	6.8	W	7.5	W	2.4	NNE
" 7	5.8	NE	7.6	N	3.0	NNE
" 8	3.0	WNW	4.2	WNW	2.9	NNE
" 9	5.0	W	6.5	W	2.5	N
" 10	6.3	W	7.0	W	1.8	NE
" 11	5.6	W	6.1	W	-	-
" 12	5.9	W	6.5	W	2.3	NNW
" 13	6.2	W	7.3	W	1.7	NNE
" 14	8.9	W	10.0	WSW	3.5	WSW
" 15	7.2	W	7.7	W	2.9	WSW
" 16	<u>5.9</u>	W	<u>6.9</u>	W	<u>1.9</u>	NW
AVE.	6.9 (m/sec)		AVE.	8.0 (m/sec)	AVE.	2.4(m/sec)
	(16 mph)			(18 mph)		(5 mph)

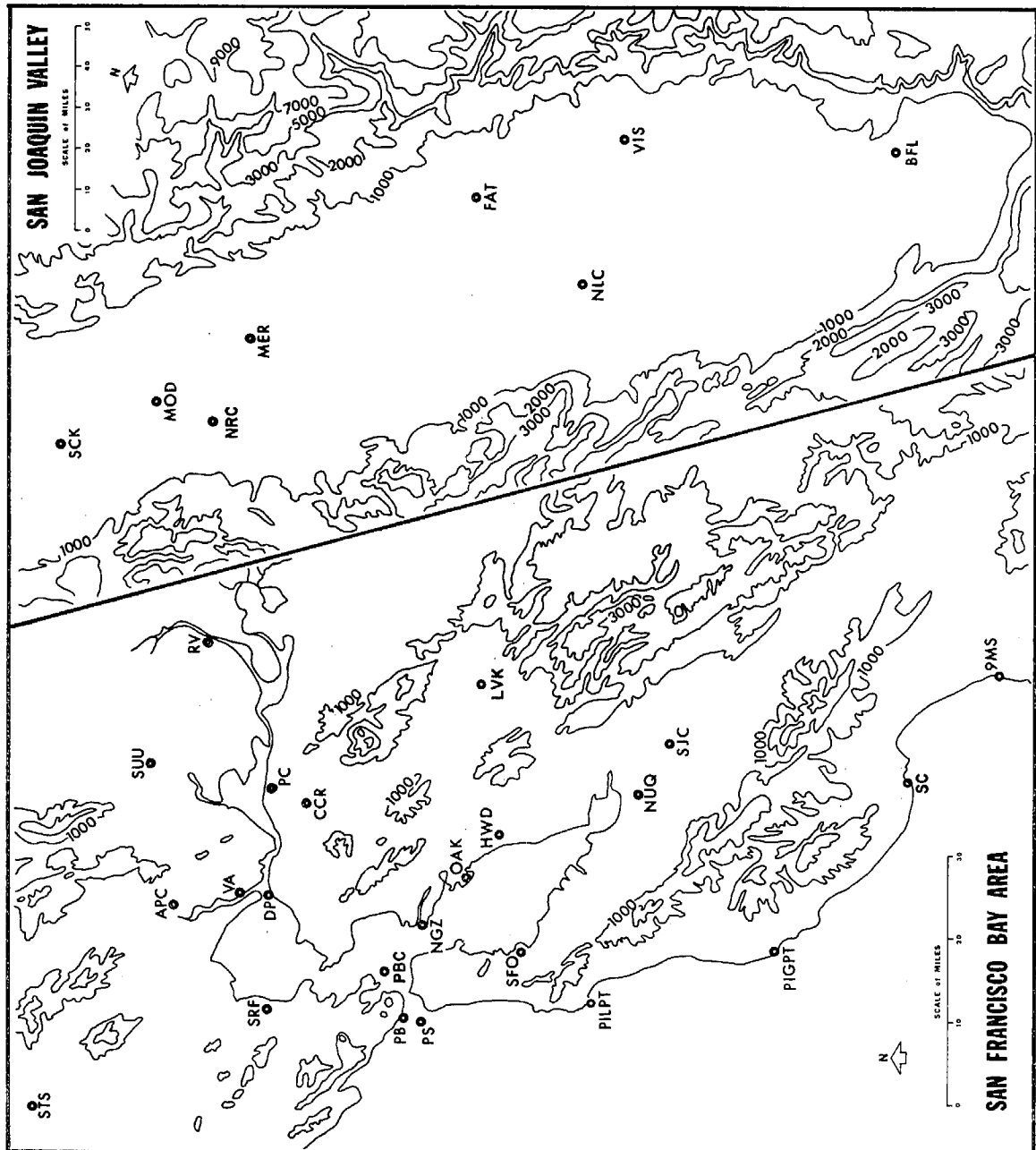


Figure 3. Topographical map of the Bay Area, California Delta, and San Joaquin Valley. Contour lines are given in feet.

lines in 1000 foot intervals for the field study region. Fosberg and Schroeder (1966) found that channeling and deflecting by topographic barriers is extremely noticeable on warm sea breeze days and to a lesser extent on cool days.

### 3. Experimental Procedure

#### 3.1 Field Test Design and Schedule

Eight tracer studies were conducted from August 31, 1976, through September 14, 1976, within the Delta Region during the four designated meteorological periods. During seven of the tests, either  $\text{SF}_6$  or  $\text{CBrF}_3$  was released from property owned by Dow Chemical in the Montezuma Hills. During the two tests where  $\text{CBrF}_3$  was used, the  $\text{SF}_6$  tracer was emitted upstream from Martinez during Test 2 and from Pinole during Test 7 in order to determine the origin and dispersion of the air passing over the Montezuma Hills. The final test involved the release of  $\text{SF}_6$  from Pinole. Releases from the Dow site covered all four meteorological periods; the releases from Martinez and Pinole were conducted during Sea Breeze and Pre-Sea Breeze conditions. The release schedule, the release locations, and tracer release rates are given in Table 2.

#### 3.2 Tracer Release System

Tracers were released at a constant rate from gas cylinders using a manifold, regulator, and large volume flowmeter; the gases were released into the air through 1/2 inch copper tubing at a height of approximately 5 meters. The release system was secured in a truck which provided an easy means of moving the release system to new release locations. Release rates were set using the regulator and calibrated flowmeter; the average release rates listed in Table 2 were determined by weighing the gas cylinders before and after each release, and averaging the weight of the released tracer over the release period. The total amount of tracer released was within 2% of the rate determined from the calibrated rotameter. The release system was continuously monitored during every release.

16  
TABLE 2

TRACER RELEASE DATA

Date	Test	Location* of SF <sub>6</sub> Release	Release Period (PDT)	Release Rate (grams/sec)	Location of CBrF <sub>3</sub> Release	Release Period	Release Rate
8/31/76	1	Montezuma Hills	1200-1700	10.6 1.01 tons/day	-	-	-
9/2/76	2	Martinez	1100-1600	11.4 1.08 tons/day	Montezuma Hills	1300-1500	16.6 1.58 tons/day
9/5/76	3	Montezuma Hills	0000-0500	9.5 0.90 tons/day	-	-	-
9/6/76	4	Montezuma Hills	1800-2300	10.8 1.03 tons/day	-	-	-
9/9/76	5	Montezuma Hills	1130-1330	10.7 1.02 tons/day	-	-	-
9/10/76	6	Montezuma Hills	0600-1100	10.5 1.00 tons/day	-	-	-
9/13/76	7	Pinole	0600-1500	11.5 1.09 tons/day	Montezuma Hills	0900-1100	16.0
						1300-1400	16.0 1.52 tons/day
9/14/76	8	Pinole	0730-1300	10.9 1.04 tons/day	-	-	-

\* Exact Tracer Release Locations: (1) Montezuma Hills: tracer was released from a truck parked by the Dow Chemical air quality monitoring station. The monitoring station is located approximately 4.3 Km east of Collinsville and 2 Km north of the Sacramento River. (2) Martinez: tracer was released from the parking lot of the Mountain View Sanitary District Sewage Plant at the end of Arthur Road. (3) Pinole: tracer was released from the parking lot of the Pinole police station on Pear Street.

### 3.3 Air Sampling Systems

#### 3.31 Automobile Traverse System

During each release day, a series of automobile air sampling traverses were conducted using from three to five, two-person teams. Automobile traverses were made by having the passenger in each car take 10-second grab samples in 30 cm<sup>3</sup> plastic syringes. Generally, samples were collected every 0.1, 0.2, 0.5 or 1.0 miles, depending upon the distance from the release point and the steadiness of the wind. Descriptions of the traverses are given in Table 3. Traverse paths were determined in the field based upon real time wind data obtained from various data collection agencies and from measurements taken by the traverse personnel. Samples taken during traverses in the early part of each test were analyzed during the test in order to determine the actual plume trajectory.

#### 3.32 Airborne Air Sampling System

Personnel from Meteorology Research, Inc. (MRI) obtained air samples in a manner similar to the automobile traverse teams from an airplane traveling downwind of the release at various heights and locations. Air samples were also obtained during spirals from above the mixing layer to the surface. Samples were typically taken at vertical intervals of 100 or 200 feet. During Test 6, Caltrans provided a plane and personnel for three airborne traverses from Sacramento to Stockton. Descriptions of the airborne traverses and spirals are also given in Table 3.

#### 3.33 Hourly Averaged Sequential Samplers

A total of 42 sequential air samplers were located at 28 sampling sites; the locations of the sites are shown in Figure 1. Samplers which

TABLE 3  
AUTOMOBILE TRAVERSES

Date	Test No.	Traverse No.	Highway	Direction Traveled	Crossroad	Traverse Time (PDT)	Distance Traveled (km)	No. Samples
8/31/76	1	1	99,120,I205	South, west	Highway 12	1400-1450	58.7	74
		2	160	South	Twitchell Island Road	1420-1433	16.7	53
		3	160	North	Highway 4	1430-1445	14.8	47
		4	160	South	Twitchell Island Road	1515-1527	14.8	47
		5	I5,120,99	East, north	Interstate 205	1600-1652	68.3	86
		6	160	North	Highway 4	1630-1641	14.8	47
		7	99,120,I205	South, west	Boessow Road (Galt)	1701-1753	70.8	89
9/2/76	2	1	I680	South	Interstate 780	1130-1143	20.0	63
		2	I680	North	Highway 24 (Walnut Creek)	1215-1228	20.0	63
		3	4,160	East, north	Loveridge Road	1240-1350	25.7	17
		4	160	North	Highway 4	1400-1415	18.7	59
		5	160	South	Highway 12	1445-1503	18.7	59
		6	160	North	Highway 4	1515-1530	18.3	39
		7	Railroad Ave.	Southwest	Highway 4	1545-1635	29.8	69
		8	Empire Mine Road	South	Lone Tree Road	1625-1640	10.4	14



TABLE 3 (cont.)

## AUTOMOBILE TRAVERSES

Date	Test No.	Traverse No.	Highway	Direction Traveled	Crossroad	Traverse Time (PDT)	Distance Traveled (km)	No. Samples
9/2/76 (cont.)	2 (cont.)	9	99, 120, 1205	South	Collier Road	1630-1715	63.6	80
		10	I580, I205, 120, 99	East, north	Foothill Road (Dublin)	1630-1737	90.9	114
		11	I205, 120, 99	East, north	MacArthur Dr.	1731-1815	63.6	80
9/5/76	3	1	160	North	Highway 4	0100-0112	18.7	59
		2	99, 120	South, west	Highway 12	0130-0210	63.6	80
		3	99	South, west	Boessow Road	0213-0259	63.6	80
		4	160	South	(Emmaton)	0240-0300	6.6	42
		5	4	West	Interstate 5	0247-0320	47.5	60
		6	160	South	Highway 12	0259-0306	5.1	65
		7	4	West	Interstate 5	0332-0415	63.6	80
		8	4, J3, 12	East, north, west	Byron Road	0414-0545	74.8	93
		9	160	North	Highway 4	0430-0445	8.9	56
		10	12, J8	East, south	Highway 160	0432-0517	38.1	80
		11	160	South	Bean pot	0441-0450	6.1	77
		12	160	North	San Joaquin River	0502-0511	7.6	48
		13	12	East	Terminus	0630-0637	8.7	18
		14	J8	North	Highway 12	0637-0647	14.5	19

TABLE 3 (cont.)

## AUTOMOBILE TRAVERSES

Date	Test No.	Traverse No.	Highway	Direction Traveled	Crossroad	Traverse Time (PDT)	Distance Traveled (km)	No. Samples
9/6/76	4	1	160	South	Highway 12	1928-1946	18.7	59
		2	99,120,1205	South, west	Highway 12	2130-2217	63.6	80
		3	160	South	Bean pot	2132-2140	6.4	80
		4	99,120,1205	South, west	Kettleman Lane	2200-2246	63.6	80
		5	160	North	San Joaquin River Bridge	2214-2222	6.3	79
		6	I205,120,99	East, north	Tracy Blvd.	2232-2320	63.6	80
		7	I205,120,99	East, north	Patterson Pass Rd. (1.4 mi e of)	2315-2400	63.6	80
9/9/76	5	1	4	East	Railroad Ave.	1255-1315	15.0	94
		2	4, 160	East, north	Railroad Ave.	1314-1330	25.4	80
		3	Sellers Rd., Cypress Rd., north Bethel Island Rd.	North, east, north	Highway 4	1349-1417	14.9	38
		4	Balfour Rd.	East	Deer Valley Rd.	1351-1405	12.1	26
		5	Marsh Creek Rd.	East	Deer Valley Rd.	1356-1428	35.7	75
		6	160,4	South, west	Twitchell Island Road	1359-1416	25.4	80
		7	Balfour Road	West	Byron Highway	1413-1426	12.1	26
		8	Balfour Road	East	Deer Valley Rd.	1436-1450	12.1	26

TABLE 3 (cont.)

## AUTOMOBILE TRAVERSES

Date	Test No.	Traverse No.	Highway	Direction Traveled	Crossroad	Traverse Time (PDT)	Distance Traveled (km)	No. Samples
9/10/76	6	1	Sherman Island Road	Southwest	160	0800-0815	5.8	37
		2	160	South	12	0740-0753	15.9	100
		3	99,120,I205	South, west	Highway 12	1001-1051	63.6	80
		4	Sherman Levee Road	South	Highway 160	1023-1033	9.5	60
		5	99	South, west	Highway 12	1030-1115	63.6	80
		6	160	North	San Joaquin River Bridge	1022-1033	6.4	80
		7	160	North	San Joaquin River Bridge	1103-1112	6.4	80
		8	I205,120,99	East, north	Patterson Pass Rd. (1.5 mi e of)	1105-1203	63.6	80
		9	I205,120,99	East, north	Tracy Blvd.	1145-1230	63.6	80
9/13/76	7	1	24,I680,I780	East, north	Highway 13	0924-0956	48.3	100
		2	Sherman Island Road	Northeast	S. end of Sherman Island Rd.	0940-1155	7.0	88
		3	12,160,4	East, south, west	Interstate 80	1113-1217	75.6	48
		4	I780,I680	South	Interstate 80	1130-1146	24.9	32
		5	I580,I205,120	East	Vasco Road	1335-1458	138.4	87
		6	I780,I680,24	South, west	Interstate 80	1340-1414	51.5	33

TABLE 3 (cont.)  
AUTOMOBILE TRAVERSES

Date	Test No.	Traverse No.	Highway	Direction Traveled	Crossroad	Traverse Time (PDT)	Distance Traveled (km)	No. Samples
9/13/76 (cont.)	7 (cont.)	7	I580	East	Highway 238	1429-1451	33.8	22
		8	I80,17,238, I580	S,S,E,E	W. Texas	1450-1706	191.5	120
			Vasco, Walnut 4,160,12	N,N N,N,W	(Fairfield)			
		9	I580	West	Highway 84	1458-1532	33.8	22
		10	24,I680,I780	East, north	Interstate 580	1537-1611	53.1	34
		11	99,120,I205, I580	S, west	Mack Road	1654-1820	132.0	83
		12	I580,17	West, north	Highway 84	1835-1901	25.7	17
9/14/76	8	1	I680	South	Interstate 80	0906-0931	38.6	49
		2	I680	North	Highway 24	0941-1007	38.6	49
		3	12,160,4,24	E,S,W,S	W. Texas Ave. (Fairfield)	1047-1151	91.7	58
		4	I680	North	Highway 24 (Walnut Creek)	1154-1220	38.6	49

TABLE 3 (cont.)

## AIRBORNE TRAVERSES AND SPIRALS

Date	Test No.	Traverse No.	Traverse Path and Direction	Altitude (meters, MSL)	Traverse Time	Distance Travelled (km)	No. Samples
9/10/76	6	1	VACA-Dixon Airport south to Isleton	305	0934-0946	38.1	11
		2	Isleton s. to 4 mi. e. of Brentwood	305	0950-1005	24.3	59
		3	4 mi. e. of Brentwood s. to I580-I205 junction	305	1012-1020	23.1	9
		4	I580-I205 junction n. to 4 mi. e. of Brentwood	183	1044-1052	23.1	8
		5	4 mi. e. of Brentwood n. to Isleton	183	1054-1107	24.3	52
		6	Isleton n. to VACA-Dixon Airport	183	1109-1122	38.1	14
		7	Isleton s. to 4 mi. e. of Brentwood	427	1140-1153	24.3	25
		8	Junction S.P.T. Co. Railroad & I580 n. to I5 and I205	305	1229-1235	17.8	7
		9	I5-I205 n. to Wilson Way & Highway 99	305	1238-1251	27.5	27
		10	Sacramento Executive Airport s. to Ripon	183	1000-1039	94.1	40
		11	Ripon n. to Sacramento Executive Airport	183	1100-1139	94.1	40
		12	Sacramento Executive Airport s. to Ripon	183	1200-1239	94.1	40

TABLE 3 (cont.)

## AIRBORNE TRAVERSES AND SPIRALS

Date	Test No.	Traverse No.	Traverse Path and Direction	Altitude (meters, MSL)	Traverse Time	Distance Traveled (km)	No. Samples
9/10/76 (cont.)	6 (cont.)	13	Ripon n. to Sacramento Executive Airport	183	1300-1339	94.1	40
9/13/76	7	1	Cordelia s. to I680 and Highway 24 (Walnut Creek)	427	0736-0748	36.5	50
		2	I680 and Highway 24 n. to Cordelia	305	0757-0810	36.5	53
		3	Cordelia s. to I680 and Highway 24	183	0819-0832	36.5	53
		4	Cordelia s. to I680 and Highway 24	427	0906-0918	36.5	12
		5	I680 & 24 to Cordelia	305	0925-0938	36.5	53
		6	Cordelia to I680 & 24	183	0945-0958	36.5	53
		7	VACA-Dixon Airport s. to Isleton	183	1112-1324	38.1	26
		8	Isleton s. to I580 & I205	183	1327-1343	47.0	62
		9	I205 & I580 n. to Isleton	305	1348-1404	47.0	68
		10	Isleton n. to VACA-Dixon Airport	305	1409-1422	38.1	27
		11	VACA-Dixon Airport s. to Isleton s. to I580 & I205	427	1428-1456	85.1	55
		12	Livermore Airport East to I5-205	457	1759-1812	44.1	27
		13	I5 & I205 Northeast to Stockton Airport	457	1815-1822	16.2	13

TABLE 3 (cont.)

## AIRBORNE TRAVERSES AND SPIRALS

Date	Test No.	Traverse No.	Traverse Path and Direction	Altitude (meters, MSL)	Traverse Time	Distance Traveled (km)	No. Samples	$\Delta H$ (meters)
9/13/76 (cont.)	7	14	Stockton Airport n. to 5.7 mi ssw of Sacramento Executive Airport	457	1850-1912	66.4	45	
9/14/76	8	1	I680-Highway 24 (Walnut Creek) n. to Cordelia	366	0826-0839	36.5	53	
		2	Cordelia s. to I680-Highway 24	274	0843-0856	36.5	53	
		3	I680-24 n. to Cordelia	183	0858-0911	36.5	53	
		4	Cordelia s. to I680-24	427	0942-0955	36.5	27	
		5	I680-24 n. to Cordelia	305	0959-1012	36.5	52	25
		6	Cordelia s. to I680-24	183	1016-1028	36.5	51	
SPIRALS								
9/10/76	6	1	Over Frank's Tract Recreation Area	914 to 488	1158-1203	-	8	61
		2	Over Frank's Tract Recreation Area	472 to 30	1203-1208	-	31	15
9/13/76	7	1	0.5 mi n. of the Port Chicago Naval Magazine	914 to 488	0845-0850	-	8	61
		2	0.5 mi n. of the Port Chicago Naval Magazine	472 to 15	0850-0854	-	33	15

TABLE 3 (cont.)

## AIRBORNE TRAVERSES AND SPIRALS

Date	Test No.	Traverse No.	Traverse Path and Direction	Altitude (meters, MSL)	Traverse Time	Distance Traveled (km)	No. Samples	$\Delta H$ (meters)
9/13/76 (cont.)	7 (cont.)	3	0.5 mi n. of the Port Chicago Naval Magazine	914 to 488	1008-1013	-	8	61
		4	0.5 mi n. of the Port Chicago Naval Magazine	457 to 0	1013-1017	-	31	15
		5	Rio Vista	1829 to 914	1518-1526	-	16	61
		6	Rio Vista	884 to 30	1526-1534	-	29	31
		7	Tracy	1829 to 914	1553-1559	-	16	61
		8	Tracy	884 to 91	1559-1603	-	27	31
		9	Stockton	1524 to 762	1832-1838	-	14	61
		10	Stockton	732 to 30	1838-1844	-	24	31
								26
9/14/76	8	1	0.5 mi n. of Port Chicago Naval Magazine	1067 to 457	0921-0926	-	11	61
		2	0.5 mi. n. of Port Chicago Naval Magazine	442 to 15	0926-0930	-	29	15
		3	0.5 mi n. of Port Chicago Naval Magazine	1372 to 457	1039-1044	-	16	61
		4	0.5 mi n. of Port Chicago Chicago Naval Magazine	442 to 15	1044-1049	-	29	15



permitted the collection of hourly averaged air samples each hour for 12 hours were positioned at 14 locations, primarily along Highway 99. An additional 14 locations along Highway 160, 10 km east of the Dow site, were designated for the positioning of battery-powered samplers which permitted the collection of hourly averaged samples each hour for three hours. These samplers were used during Tests 1 and 2. Table 4 lists the site locations, crosswind distances from a reference point and downwind distances from the three release points.

#### 3.4 Chemical Analysis of Air Samples

Air samples were analyzed for  $\text{SF}_6$  and  $\text{CBrF}_3$  using electron capture gas chromatography. The tracers were separated in a stainless steel column (39" x 0.25" OD, 0.18" ID) packed with 80-100 mesh 5A Molecular Sieve. Prepurified nitrogen flowing at 10 psig, caused the  $\text{SF}_6$  to elute in 18 seconds and the  $\text{CBrF}_3$  to elute in 40 seconds. Both column and detector were operated at ambient temperatures. A typical chromatogram is shown in Figure 4; additional details concerning the gas chromatographs are available elsewhere (Drivas, 1974).

Twelve chromatographs and two digital integrators were set up in a room at the California Holiday Lodge, Fairfield, California. Only eight of the chromatographs were used during the test; four were used to analyze for  $\text{SF}_6$  alone and four were set up to analyze for both tracers. Field samples were returned each day to the lab for analysis. All of the samples from one test were analyzed before the next test began. Calibration was done using an exponential dilution method. Calibration results show that concentrations down to  $10^{-12}$  parts  $\text{SF}_6$  per part air and  $10^{-11}$  parts  $\text{CBrF}_3$  per part air could be detected at a signal-to-noise ratio of

28  
TABLE 4

LOCATION OF HOURLY AVERAGE SEQUENTIAL SAMPLERS

Hourly Average 12-Hour Sequential Sampling Stations

Location of 12-Hour Samplers	<u>Distance from Release Points (Km)</u>			Distance S. of Sacramento (Km)
	Montezuma Hills	Martinez	Pinole	
1 Fairfield	28.6	28.1	36.0	-
2 Davis	50.4	64.6	73.7	-
3 Sacramento	61.1	81.1	92.5	0
4 Elk Grove	59.3	84.4	99.6	18.0
5 Herald	54.0	80.6	96.3	29.9
6 Collier Road	48.9	75.8	92.0	39.3
7 Lodi	46.6	73.2	90.2	49.9
8 Hammer Lane	41.3	66.6	83.9	62.7
9 Stockton	48.7	73.2	90.0	67.0
10 French Camp	51.9	74.5	91.5	76.0
11 Manteca	59.3	79.6	96.3	84.8
12 Tracy	61.8	77.5	93.0	99.3
13 Livermore	44.3	47.1	59.5	-
14 Rio Vista	13.4	39.0	55.0	-

29  
TABLE 4 (cont.)

3-hour Boards	<u>Distance from Release Points (Km)</u>		Distance N. of Highway 4 - Highway 160 Junction (Km)
	Montezuma Hills	Martinez	
1	12.2	36.2	26.4
2	12.9	37.5	23.8
3	12.9	38.3	22.2
4	13.7	39.5	30.0
5	12.4	38.3	17.9
6	10.9	37.0	15.0
7	9.4	35.5	13.4
8	8.1	34.2	10.9
9	5.8	31.4	8.8
10	6.1	30.9	7.4
11	7.6	31.2	6.1
12	7.1	29.1	4.2
13	8.4	28.6	4.2
14	9.4	26.1	3.4 (south of 4&160)

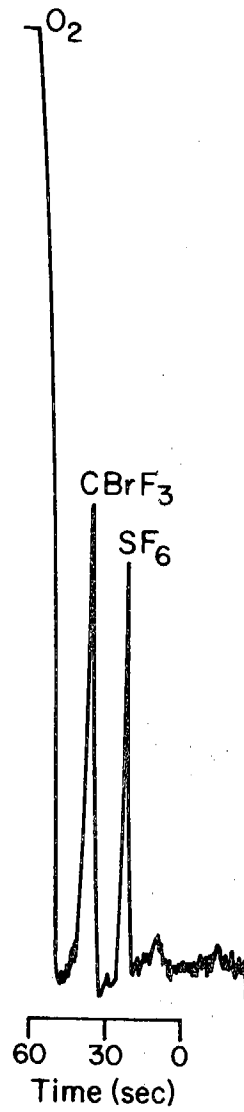


Figure 4. Typical tracer chromatogram:  $[SF_6] = 6$  ppt;  $[CBrF_3] = 310$  ppt.

better than 3 to 1. A typical calibration curve is shown in Figure 5. The chromatogram peaks were integrated with an Autolab System I electronic digital integrator (Spectra-Physics, Santa Clara, California). The gas chromatographs were calibrated before and after the field test period. During the tests, the instruments were cross-checked periodically for reproducibility. The calibration of the tracer data changed by approximately 7% among the gas chromatographs used to analyze  $\text{SF}_6$  alone. Calibration results for the remaining gas chromatographs changed by 25% for  $\text{SF}_6$  and 20% for  $\text{CBrF}_3$ . Degradation of the columns and detectors due to atmospheric contaminants in the air samples is the probable cause for the changes in the calibration results. Previous experience has shown that the presence of halogenated solvents in air samples can, over an extended period of use of the chromatograph, contaminate the detector and column. Uncertainty in the tracer data is estimated to range from less than 5% to no more than 25%. Details of the calibration results are given in Appendix A of this volume.

### 3.5 Meteorological Support Systems

#### 3.51 Surface Wind Data

Data obtained from MRI were collected from the various agencies listed in Table 5. Table 5 also contains stations maintained by the Bay Area Air Pollution Control District and various industrial companies. The data for these stations were obtained directly from the Bay Area APCD. The data for each station during the test period are tabulated in Table 17 of Volume II, Part B. Measurements from 27 of the 36 wind stations provided hourly averaged wind direction and velocity data; 3 stations measured 2 or 3-hour averaged data. Data from the remaining 6 stations were recorded as single hourly observations. The locations of the stations are shown in Figure 6.

#### 3.52 Upper Air Wind Data

Pilot balloon upper air wind speed and direction measurements (pibal measurements) were taken by MRI at the times and locations indicated in Table 5. The data obtained from these measurements are given in Table 18 of Volume II, Part B. MRI also provided estimates of the mixing depth at various locations and times during the test based upon upper air wind and temperature measurements. These data are given in Table 19 of Volume II, Part B. Vector-averaged wind speed and direction data from the surface to the height of the mixing layer are given in Table 20 of Volume II, Part B. The locations of the upper air stations are shown in Figure 6.

34  
TABLE 5

WIND DATA STATIONS AND DESCRIPTION OF WIND DATA

Station	Station Code	Description of Data
1 Dow Surface (Rockwell)	DW01	Hourly averaged wind speed, wind direction at 5-minute intervals
2 Brentwood (Rockwell)	BR02	Hourly averaged wind speed, wind direction at 5-minute intervals
3 Venice Ferry (MRI)	VF03	Hourly averaged speed and direction
4 Rio Cosummes (MRI)	RC04	Hourly averaged speed and direction
5 Stockton (NWS)	SK05	Single hourly observations
6 Livermore (NWS)	LV06	Single hourly observations
7 Rio Vista (NWS)	RV07	Single hourly observations
8 Sacramento (Metropolitan Airport) (NWS)	SA08	Single hourly observations
9 Concord (Buchanan Field) (NWS)	CC09	Single hourly observations
10 Benicia (BAAPCD)	BE10	Hourly averaged speed and direction
11 Voice of America Radio Tower	VA11	Hourly averaged speed and direction
12 Pittsburg PG&E Company	PB12	Hourly averaged speed and direction
13 Martinez Shell Oil	MZ13	Hourly averaged speed and direction
14 Martinez Lion Oil	MZ14	Hourly averaged speed and direction
15 Antioch Fibreboard	AT15	Hourly averaged speed and direction

TABLE 5 (cont.)

Station	Station Code	Description of Data
16 Benicia Exxon	BE16	Hourly averaged speed and direction
17 Richmond Allied Chemical	RM17	Hourly averaged speed and direction
18 Pittsburg Allied Chemical	PB18	Hourly averaged speed and direction
19 Rodeo Union Oil	RD19	Hourly averaged speed and direction
20 Concord BAAPCD	CC20	Hourly averaged speed and direction
21 Vallejo BAAPCD	VL21	Hourly averaged speed and direction
22 San Rafael BAAPCD	SR22	Hourly averaged speed and direction
23 San Francisco BAAPCD	SF23	Hourly averaged speed and direction
24 Redwood City BAAPCD	RC24	Hourly averaged speed and direction
25 Livermore BAAPCD	LV25	Hourly averaged speed and direction
26 Fremont BAAPCD	FR26	Hourly averaged speed and direction
27 Pittsburg BAAPCD	PB27	Hourly averaged speed and direction
28 Rancho Seco Nuclear Power Plant Site	RS28	Hourly averaged speed and direction
29 Sacramento Caltrans	SA29	Hourly averaged speed and direction
30 Davis Caltrans	DV30	Hourly averaged speed and direction



TABLE 5 (cont.)

Station	Station Code	Description of Data
31 Wilton Caltrans	WT31	Hourly averaged speed and direction
32 Rio Vista Yolo-Solano APCD	RV32	3-Hourly averaged speed and direction
33 Woodland Yolo-Solano APCD	WD33	2-Hourly averaged speed and direction
34 Davis Yolo-Solano APCD	DV34	2-Hourly averaged speed and direction
35 Stockton San Joaquin APCD	SK35	Miles of wind/hr by quadrant
36 Travis Travis Air Force Base	TR36	Single hourly observations

37  
TABLE 5 (cont.)

UPPER AIR WIND SPEED AND DIRECTION MEASUREMENTS

Station	Station Code	Date and Time (PDT)	
Dow Tower	DW50	Continuous 8/31/76 through 9/14/76	
Dow Pibal	DW51	8/31/76	1100-1700
		9/2/76	1000-1700
		9/5/76	0000-0500
		9/6/76	1700-2300
		9/9/76	1100-1400
		9/10/76	0700-1200
		9/13/76	0700-1700
		9/14/76	0800-1600
B & W Resort Pibal	BW52	8/31/76	1000-1800
		9/2/76	1000-1800
		9/5/76	0000-0600
		9/6/76	1600-2400
		9/9/76	1000-1400
		9/10/76	0800-1900
Livermore Pibal	LV53	8/31/76	1000-1800
		9/2/76	0900-1000
		9/9/76	0900-1900
		9/10/76	1100-1800
		9/13/76	0800-1800
		9/14/76	0800-1500
Pinole Pibal	PN54	9/13/76	0600-1600
		9/14/76	0600-1700
Junction J2 & CAL4 Pibal	JC55	9/14/76	1600-1900
Benicia Pibal	BE56	9/10/76	1400
Rancho Seco Nuclear Power Plant Site Tower	RS57	Continuous at 200 feet, hourly standard deviation of the wind	
Oakland International Airport Pibal	OK58	8/31/76 through 9/14/76 2 measurements per day	

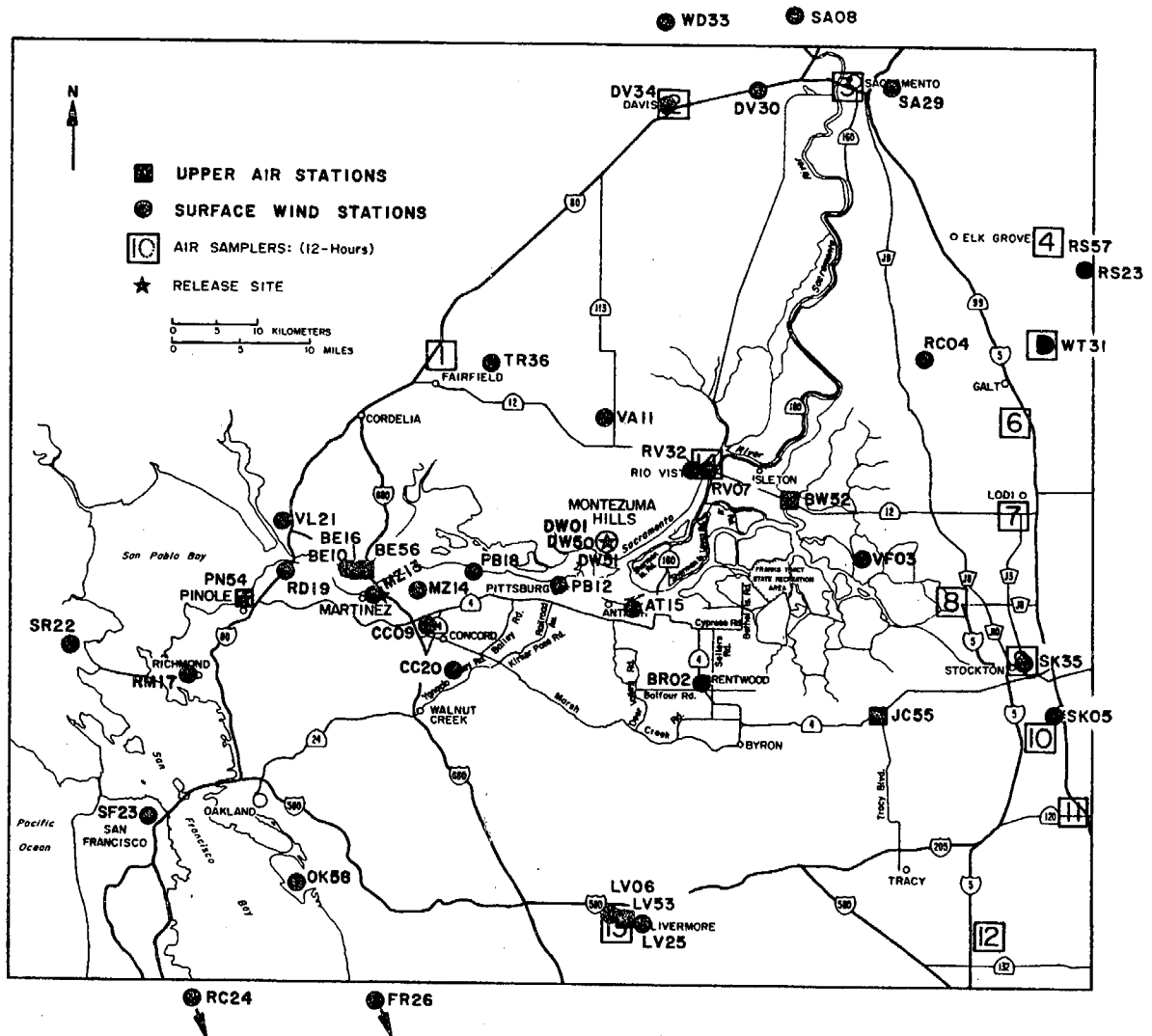


Figure 6. Location of surface wind and upper air data stations.

#### 4. Presentation and Discussion of Results

The tracer and meteorological data have been presented graphically in Volume II, Part A, and tabulated in Volume II, Part B, of this report. Results from a portion of the data reduction procedures are also given in Volume II, Part A. In the remainder of this volume, we will present detailed summaries of the qualitative and quantitative results of each test period; we will examine and discuss the atmospheric dispersion characteristics of the Delta Region, and perform a consistency check of the tracer data based on mass balance considerations. We will seek to determine the applicability of the Gaussian plume model to the description of pollutant impact within the test region, and we will present an important relationship between the standard deviation of the wind direction and the Gaussian horizontal dispersion parameter.

##### 4.1 Relation of Tracer Data to Industrial Pollutant Emissions

As a means of interpreting the results of the California Delta tracer tests in terms of existing or projected industrial pollutant emissions, we have developed a simple nomograph to be used to convert measured tracer concentrations to pollutant concentrations. Such a conversion necessarily implies that the pollutant emissions of interest are suitably characterized by the tracer release. The conversion of concentrations also implies that either the pollutant is essentially unreactive (like the tracer) or that its rate of reaction is very rapid. For example, carbon monoxide may be considered unreactive over the time scale involved in tracer transport. Sulfur dioxide has been shown to have a relatively slow (15%/hr) reaction rate (Roberts, 1975); nitrogen oxide (NO) can be converted rapidly to nitrogen dioxide (NO<sub>2</sub>) in the

presence of high oxidant concentrations. In cases like  $\text{SO}_2$ , the conversion of tracer concentrations to pollutant concentrations gives an upper bound on the pollutant concentration. If, as in the example of  $\text{NO}$ , a pollutant reacts fairly rapidly, then the conversion of tracer concentrations to the product concentrations ( $\text{NO}_2$ ) will yield an upper bound on the product concentrations.

The tracer concentrations obtained during the California Delta field study can be converted to pollutant concentrations using the nomographs in Figures 7 and 8. In order to use the nomographs, a value of  $K$ , the ratio of the pollutant molecular weight (in grams) to the pollutant's existing or projected emission rate (in tons/day) must be specified. Any tracer concentration measured during the Delta field study can then be converted to the concentration of the pollutant by selecting the point along the specified  $K$ -line where the tracer concentration occurs. As examples, the projected emissions of  $\text{NO}_x$  (as  $\text{NO}_2$ ),  $\text{SO}_2$  and  $\text{CO}$  associated with the Dow complex have been used to specify the  $K$ -lines which are shown in the nomographs. A concentration of 100 ppt  $\text{SF}_6$  converts to 2.93 ppb  $\text{NO}_2$ , .242 ppb  $\text{SO}_2$ , and .499 ppb  $\text{CO}$ . In the case of  $\text{NO}_2$  we have assumed that  $\text{NO}$  reacts rapidly to form  $\text{NO}_2$ . A summary of the preliminary estimates of emissions from the Dow project are given in Table 6 (Moyer, 1977). A more detailed list is tabulated in Volume II, Part A, Table 6.

The nomographs are based upon the following equation:

$$[P] = [T] \cdot \frac{MW_T}{RR_T} \cdot \frac{RR_P}{MW_P} = [T] \cdot \frac{K_T}{K_P} \quad (1)$$

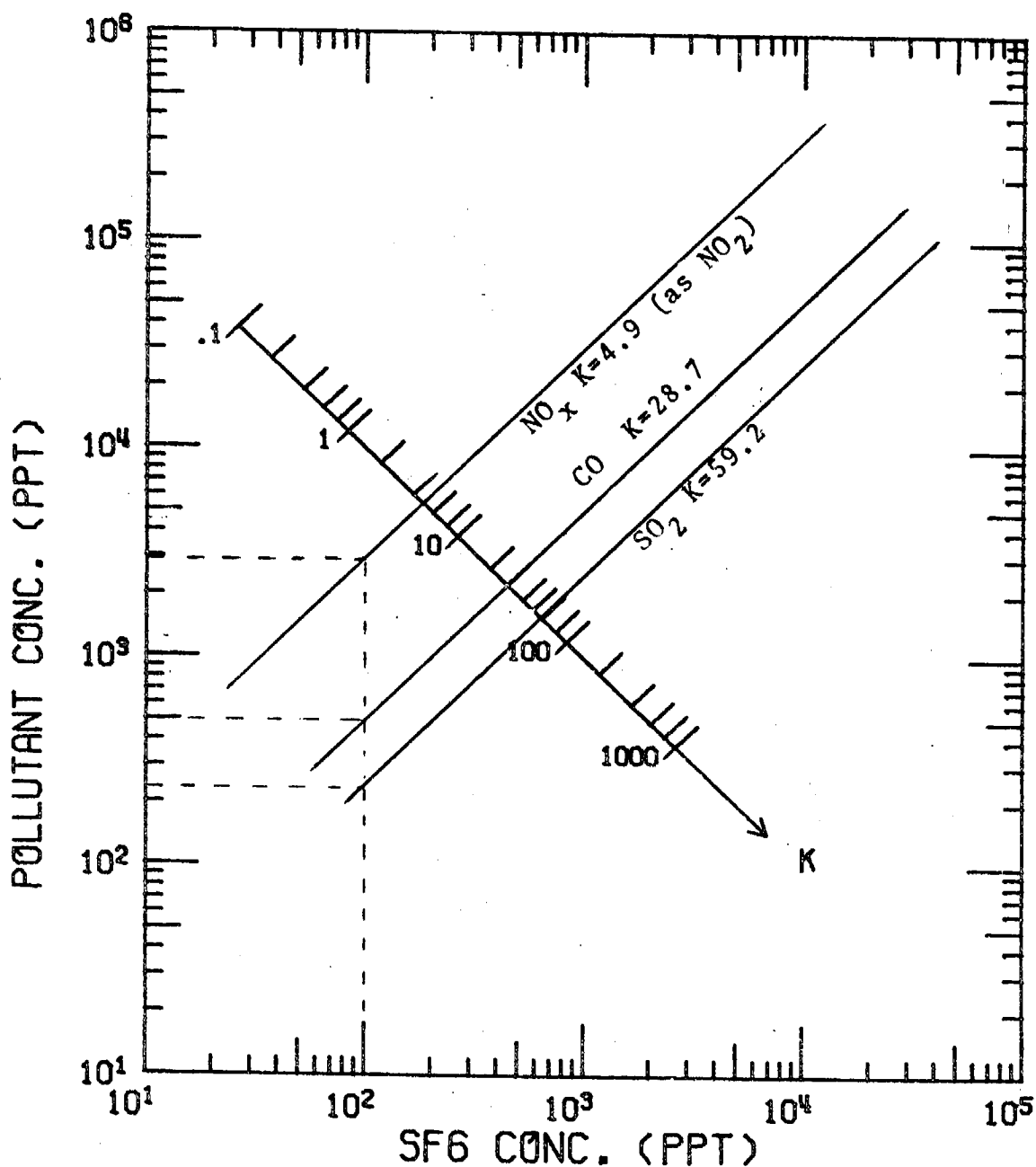


Figure 7. Conversion nomograph for converting SF<sub>6</sub> tracer concentrations measured during the field study to pollutant concentrations.  $K = (\text{pollutant molecular wt., grams}) / (\text{pollutant emission rate, tons/day})$ . Values of K shown above are based on projected pollutant emissions from the Montezuma Hills Dow chemical complex. Dashed line indicates the corresponding tracer-to-pollutant concentration conversions.

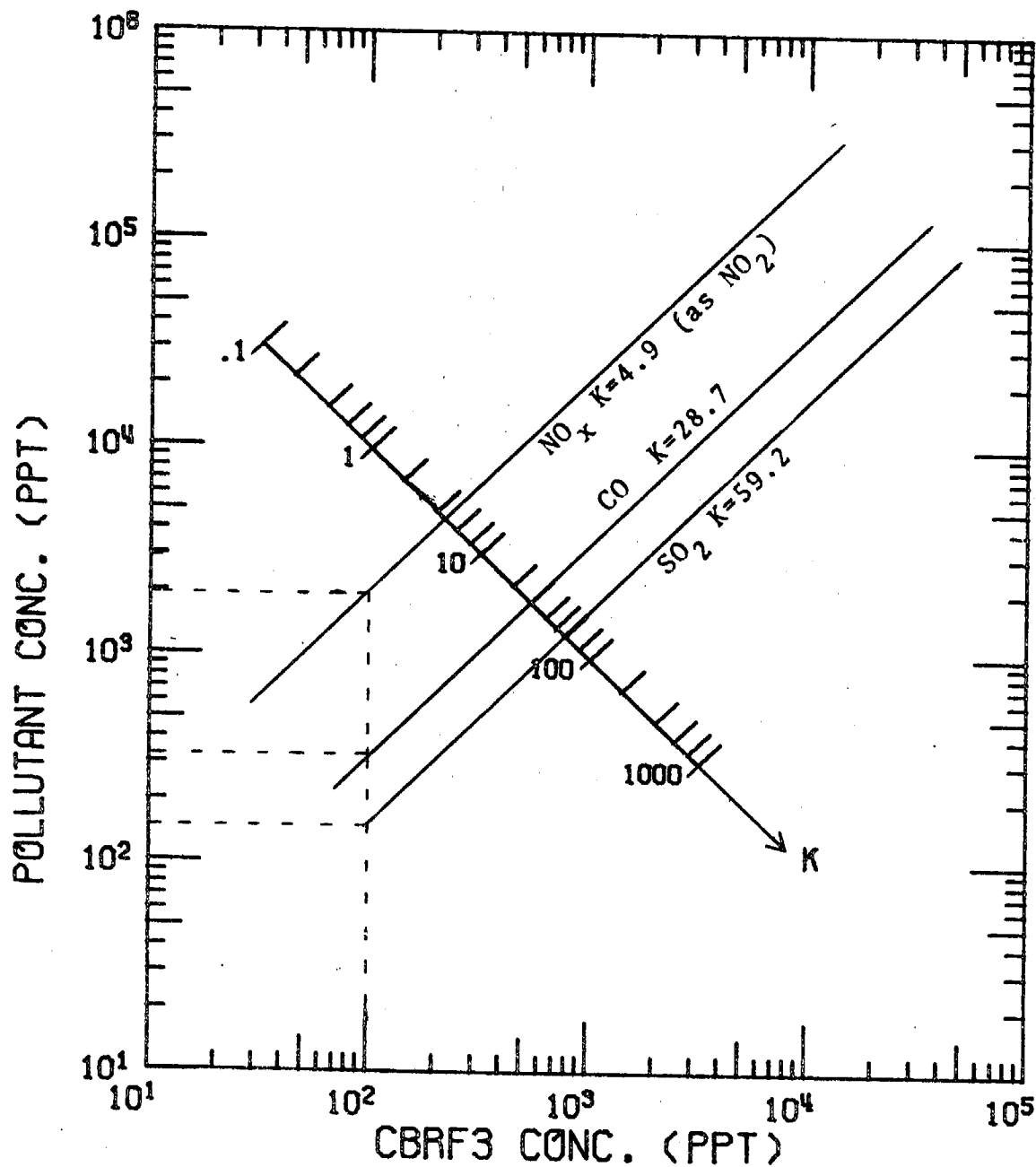


Figure 8. Conversion nomograph for converting CBrF<sub>3</sub> tracer concentrations measured during the field study to pollutant concentrations.  $K = (\text{pollutant molecular wt, grams}) / (\text{pollutant emission rate, tons/day})$ . Values of K shown above are based on projected pollutant emissions from the Montezuma Hills Dow chemical complex. Dashed line indicates the corresponding tracer-to-pollutant concentrations conversions.

TABLE 6  
NOMOGRAPH K-VALUES FOR PROJECTED DOW EMISSIONS\*

$$K \equiv \frac{\text{Mol. Wt. of Pollutant (grams)}}{\text{Emission Rate (tons/day)}} = \frac{MW_p}{RR_p}$$

Pollutant	MW <sub>p</sub> (grams)	RR <sub>p</sub> <sup>*</sup> (tons/day)	K Dow only	RR <sub>p</sub> <sup>**</sup> Dow + Turbine	K Dow + Turbine
NO <sub>x</sub> (as NO <sub>2</sub> )	46	9.41	4.89	23.10	1.99
SO <sub>2</sub>	64	1.08	59.2	1.252	51.12
CO	28	0.976	28.68	4.796	5.84
NMHC <sup>+</sup>	-	1.516	-	2.900	-

MW<sub>p</sub> = molecular weight of pollutant (grams/mole)

RR<sub>p</sub> = emission rate of pollutant (tons/day)

\* Projected Dow emissions for Montezuma Hills chemical complex from Moyer (1977).

\*\* Plans concerning the development of the Dow project indicated a 146 megawatt gas turbine might be necessary as an on-site power source. The emissions resulting from the operation of such a turbine were obtained from Moyer (1977).

+ Values of K for nonmethane hydrocarbons (NMHC) have not been calculated because the complex reaction mechanisms prevent simple descriptions of the rates of conversion.



where  $[P]$  is the pollutant concentration in ppt,  $[T]$  is the tracer concentration in ppt,  $RR_T$  and  $RR_P$  are the tracer and pollutant release rates in tons/day, respectively, and  $MW_T$  and  $MW_P$  are the associated molecular weights in grams. The terms  $K_T$  and  $K_P$  are the respective ratios of tracer and pollutant molecular weights to emission rates. The K-lines shown in the nomographs are based on the average tracer release rates during the eight tests (1.02 tons  $SF_6$ /day, 1.55 tons  $CBrF_3$ /day). This introduces only a small error (4%) since the release rates were relatively constant from test to test.

Table 7 gives an indication of how emissions from existing sources in the northern Bay Area and near the Montezuma Hills compare with the projected Dow emissions. Pollutant emission rates and the corresponding values of K are listed for the major point sources in the region of interest. These emission rates were taken from the Bay Area APCD Emissions Inventory Summary Report (Base Year, 1975), (Moyer, 1977). We have listed the calculated values of K for these sources as a comparison to the Dow values. Using these values of K to predict pollutant concentrations due to any of the listed sources can only yield a very rough approximation. The tracer source characteristics, in general, may be expected to differ in several important aspects from the source characteristics of these industrial facilities. The effects of the exact location, stack height, or stack velocity are difficult to extrapolate without additional experimental data.

TABLE 7

## POLLUTANT EMISSIONS FROM MAJOR POINT SOURCES IN THE NORTHEASTERN BAY AREA

The following list shows the larger point sources and their annual average emissions for 1975. The emissions shown are the total for the whole source site.

The symbol (--) indicates a quantity less than 0.01 Tons/Day.

1975 MAJOR SOURCES (NORTHEASTERN BAY AREA APCD)	ANNUAL AVERAGE EMISSIONS (T/D) AND NOMOGRAPH K-VALUES (K = MOLECULAR WT./EMISSION RATE)						
	ORG	NOX	KNOX	SO <sub>2</sub>	KSO <sub>2</sub>	CO	KCO
ALLIED CHEMICAL CORP. BAY POINT	.04	.04	1200	5.6	11	.6	47
ANTIOCH BUILDING MATERIALS PITTSBURG	.05	.01	4600	---		.2	140
ATLANTIC RICHFIELD BULK PLANT, RICHMOND	.7	---	----	---	--	--	---
CALIFORNIA & HAWAIIAN SUGAR CO., CROCKETT	.04	2.5	18	---	--	.3	93
CHEVRON CHEMICAL CO. RICHMOND	.2	.06	770	.03	2100	.2	140
COLLIER CARBON & CHEM. CORP., NICHOLS	--	2.1	22	4.1	16	--	---
CROWN-ZELLERBACH CORP. ANTIOCH	0.1	.8	58	.02	3200	--	---
CROWN CORK & SEAL RICHMOND	.7	.03	1500	--	--	.04	700
DOW CHEMICAL COMPANY PITTSBURG	.3	4.0	12	.09	710	1.6	18
E. I. DUPONT COMPANY ANTIOCH	.4	.5	92	--	19	1.5	---
EXXON CO., U.S.A. BENICIA	9.1	9.8	4.7	40	1.6	4.2	6.7

NO<sub>x</sub> emissions are assumed to be in terms of tons NO<sub>2</sub>/day.

1975 MAJOR SOURCES (NORTHEASTERN BAY AREA APCD)	ANNUAL AVERAGE EMISSIONS - T/D						
	ORG	NOX	KNOX	SO <sub>2</sub>	KSO <sub>2</sub>	CO	KCO
EXXON CO., U.S.A. BULK PLANT, BENICIA	.3	---	---	---	---	--	---
FIBREBOARD CORP. ANTIOCH	.6	.8	58	.03	2100	22	1.3
GLASS CONTAINERS CORP. ANTIOCH	---	.5	92	.2	320	--	---
GULF OIL CO. - CALIF. BULK PLANT, HERCULES	2.5	1.3	35	.4	160	--	---
GULF OIL CO. - CALIF. BULK PLANT, HERCULES	3.1	---	---	--	---	--	---
HERCULES INC. HERCULES	.02	.5	92	--	---	--	---
JOHNS-MANVILLE CORP. PITTSBURG	--	.1	460	--	---	--	---
MARE ISLAND NAVAL SHIPYARD VALLEJO	.4	.8	58	.03	2100	.04	700
MARTINEZ PETROLEUM BULK PLANT, MARTINEZ	.08	--	---	--	---	--	---
MONSANTO COMPANY MARTINEZ	--	.3	150	26	2.5	2.2	13
MYERS DRUM COMPANY SAN PABLO	.3	.01	4600	--	---	--	---
PACIFIC GAS & ELECTRIC CO. (AVON PLANT), AVON	.01	3.7	12	2.8	23	--	---
PACIFIC GAS & ELECTRIC CO. (CONTRA COSTA PLANT), ANTIOCH	.06	11	4.2	5.4	12	.01	2800
PACIFIC GAS & ELECTRIC CO. (PITTSBURG PLANT) PITTSBURG	.1	34	1.4	14	4.6	.03	930
PHILLIPS PETROLEUM CO. MARTINEZ	14	9.2	5.0	18	3.6	.08	350
PHILLIPS PETROLEUM CO. BULK PLANT, MARTINEZ	.4	--	---	--	---	--	---

1975 MAJOR SOURCES (NORTHEASTERN BAY AREA APCD)	ANNUAL AVERAGE EMISSIONS - T/D						
	ORG	NOX	KNOX	SO <sub>2</sub>	KSO <sub>2</sub>	CO	KCO
QUARRY PRODUCTS, INC. RICHMOND	--	.02	2300	--	---	--	---
RADIANT COLOR CO. RICHMOND	.2	--	---	--	---	--	---
SAFEWAY STORES, INC. (HOFFMAN BLVD), RICHMOND	.3	.02	2300	--	---	--	---
SHELL OIL COMPANY MARTINEZ	20	6.9	6.7	11	5.8	4.7	6.0
STANDARD OIL CO. OF CALIF., RICHMOND	22	20	2.3	12	5.3	9.8	2.9
STANDARD OIL CO. OF CA. BULK PLANT, AVON	.3	--	---	--	---	--	---
STANDARD OIL CO. OF CA. BULK PLANT, RICHMOND	.5	--	---	--	---	--	---
STAUFFER CHEMICAL CO. MARTINEZ	--	.05	920	7.9	8.1	.1	280
TEXACO, INC. BULK PLANT, RICHMOND	.4	--	---	--	---	--	---
UNION OIL CO. OF CALIF. RODEO	10	5.1	9.0	8.2	7.8	1.4	20
UNION OIL CO. OF CALIF. BULK PLANT, RICHMOND	.6	--	---	--	---	--	---
U. S. STEEL CORP. PITTSBURG	.02	.6	77	--	---	.04	700

#### 4.2 Description of the Tracer Tests

In this section, a brief synopsis of each tracer test will be presented. The purpose of the test, the test schedule, and the test meteorology will be outlined; typical results for each test will be presented in the form of overview maps of the automobile and airborne traverse data and the hourly averaged data.

Turner's (1961) method of determining stability class based upon wind speed and insolation was used to classify the stability for each test period. The average insolation or cloud cover, the average wind speed, the average mixing layer depth, and the resulting stability class are given in Table 8. The average wind vector at the tracer release point during the release period is also given.

##### 4.21 Tracer Test 1 (8/31/76)

The purpose of the first tracer test was to probe the transport and dispersion of pollutants emitted from the Montezuma Hills under afternoon Sea Breeze conditions.  $SF_6$  was released at a steady rate of 10.6 g/sec (1.10 tons/day) from 1200 to 1700 PDT.

The average wind vector at the Dow site during the release was  $270^\circ$  at 5.3 m/sec; the overall average wind for the area during the afternoon was  $300^\circ$  at 3.4 m/sec. The sky was clear, and Pasquill classes B-C were assumed to exist. The average standard deviation of the wind at Dow was  $9^\circ$ . The average mixing height during the test was approximately 960 meters, and maximum mixing height reached 2300 m after 1500 PDT. The wind pattern observed at 1600 PDT shown in Figure 9 is typical of the afternoon. The pattern appears to be similar to the Smalley wind flow type NW-5; this pattern occurred 13% of the time in August and

TABLE 8

## AVERAGE METEOROLOGICAL CONDITIONS DURING FIELD TESTS

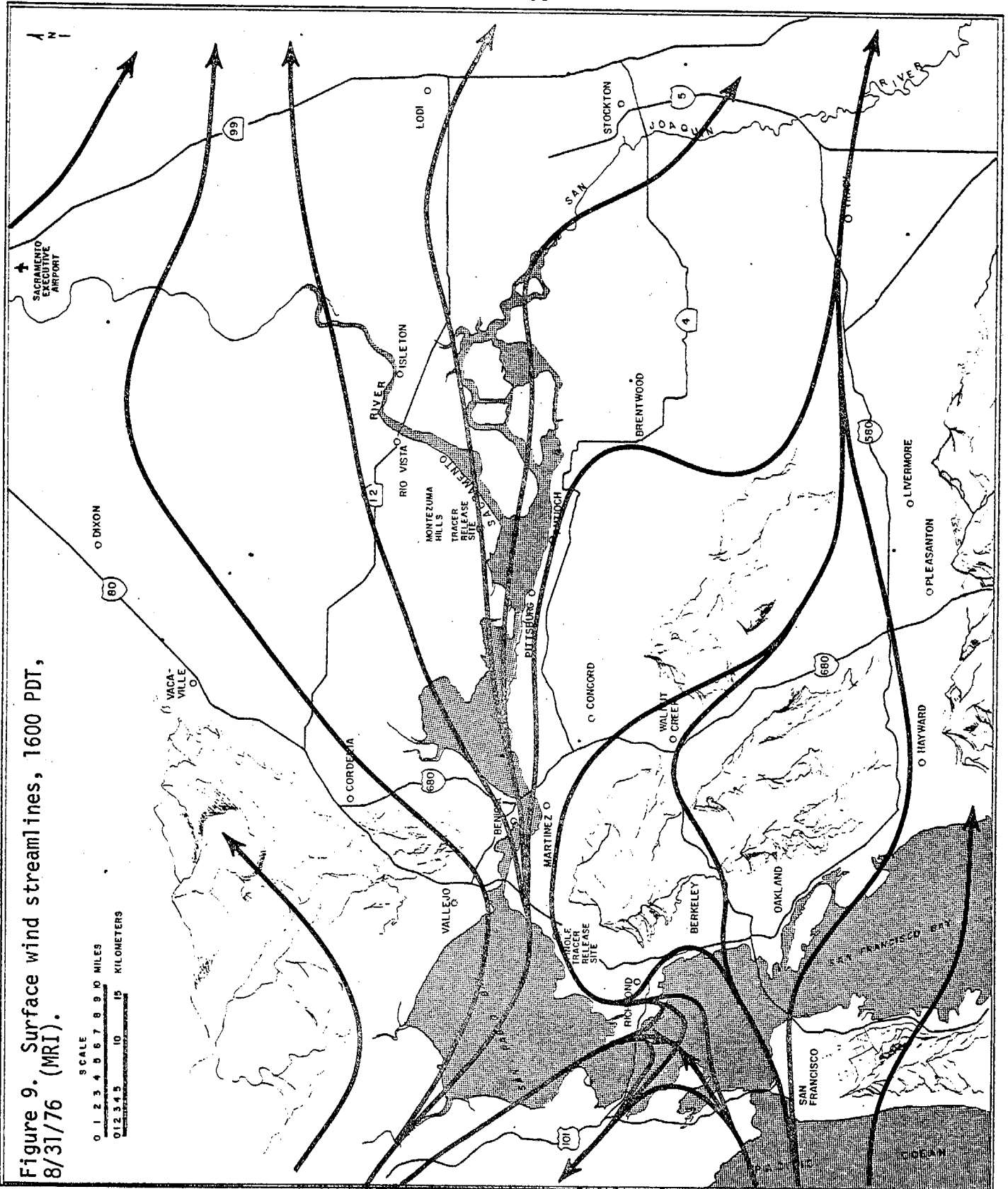
Test	Time PDT	$L^*$ m	$u^{**}$ deg/m/sec	$u_r^{***}$ (release point)	Cloud cover	Stability class
1	1200-1800	960	300/3.4	270/5.3	clear	B-C
2	1100-1700	830	290/4.3	270/4.0 (Mart.)	clear	B-C
	1300-1500			270/9.2 (Dow)		
3	0000-0600	860	290/3.3	280/9.3	scattered	D-F
4	1800-0000	510	290/3.3	280/7.1	broken	D-F
5	1100-1500	1910	340/2.6	17/1.8	scattered	B-C
6	0600-1400	1250	270/1.2	280/6.3	overcast	D
7	0600-1900	830	280/2.3	240/2.6 (Pinole)	scattered	B-C
				270/4.6 (Dow)		
8	0700-1300	1200	250/3.6	220/3.7	scattered	B-C

\* The average height of the mixing depth,  $L$ , was calculated from available hourly mixing depths for all stations over the indicated time period.

\*\* The average wind direction and speed was obtained by vector averaging data from all downwind stations over the time indicated.

\*\*\*  $u_r$  is the average wind direction and speed at the tracer release point during the time of the release. Surface data from Rodeo (4 Km northeast of Pinole) were used for determining  $u_r$  at Pinole.

Figure 9. Surface wind streamlines, 1600 PDT, 8/31/76 (MRI).



6% of the time over a year in the Smalley study. A quantitative description of the Test 1 wind patterns and tracer trajectories based upon a numerical solution of the mass balance equation is given in Section 5 of this volume. Peak ozone concentrations in the area reached .16 ppm at Livermore during the afternoon.

Four automobile traverses were conducted along Highway 160 7 km downwind between 1420 and 1641 PDT. The plume crossed Highway 160 approximately 9 km north of the Highway 160-Highway 4 junction. Peak concentrations observed in the traverses ranged from 611 ppt to 1223 ppt. Three automobile traverses were conducted along Highway 99 from Galt to Tracy; the two traverses conducted between 1400 and 1700 PDT indicated the plume had not yet crossed Highway 99. Traverse 7, conducted from 1701 to 1753 PDT, showed the center of the plume, 52 km downwind, to be 6 km east of Tracy at the intersection of I5 and I205. The plume had a centerline concentration of 64 ppt and an observable width of approximately 39 km. Traverses 6 and 7 are shown in Figure 10. As indicated in Traverse 7, emissions from the Dow site ultimately can impact in the San Joaquin Valley, south of Tracy. The average wind speed associated with the transport of the plume from the Montezuma Hills to Highway 99 was about 3 m/sec.

Hourly averaged samples were collected at points along Highway 160 and Highway 99. Peak hourly concentrations along the two routes were 636 ppt and 103 ppt, respectively. The hourly averaged plume crossing Highway 160, 7 km downwind, was centered 8.8 km north of the Highway 160-Highway 4 junction and was approximately 5.6 km wide; hourly crosswind profiles are shown in Figure 11. Further downwind at 45 km, the



TEST 1  
8/31/76

6 1630 - 1641 PDT, SF<sub>6</sub>(max) = 1223 ppt  
7 1701 - 1753 PDT, SF<sub>6</sub>(max) = 64 ppt  
SF<sub>6</sub> released from the Montezuma Hills from 1200-1700 PDT.

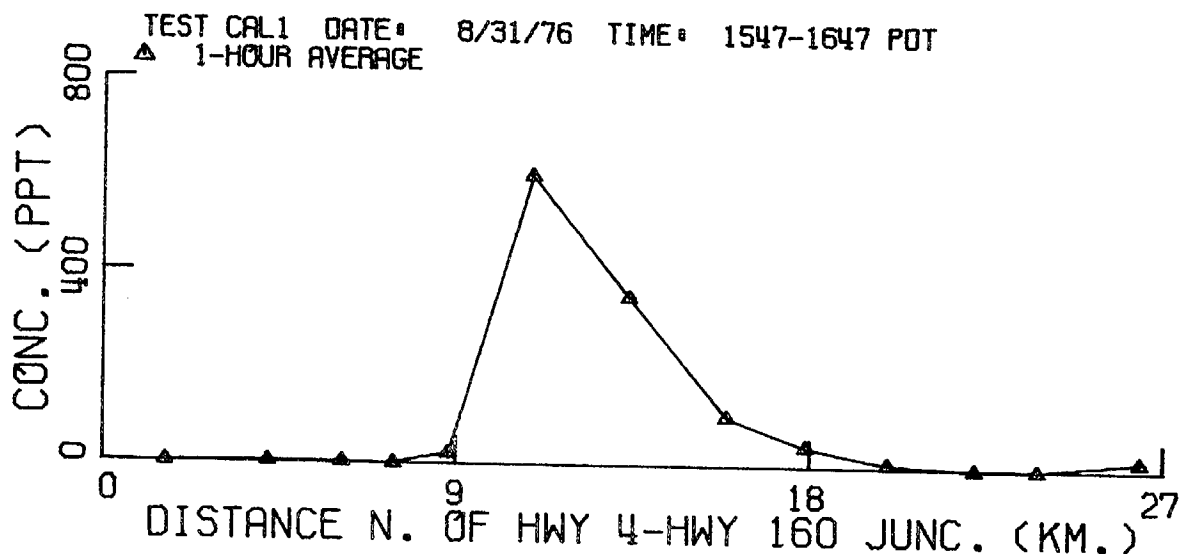
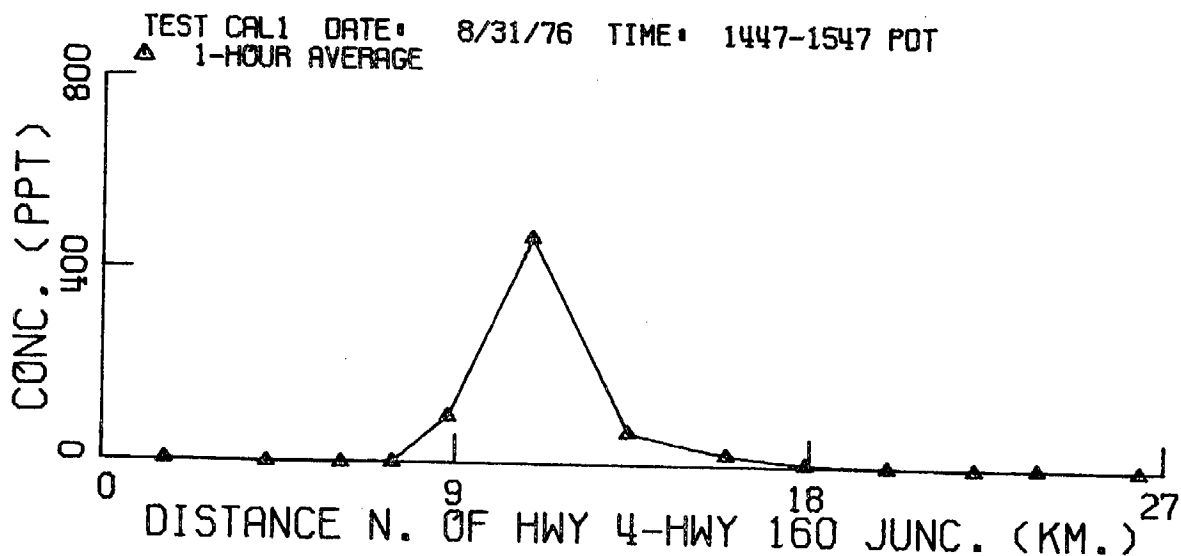
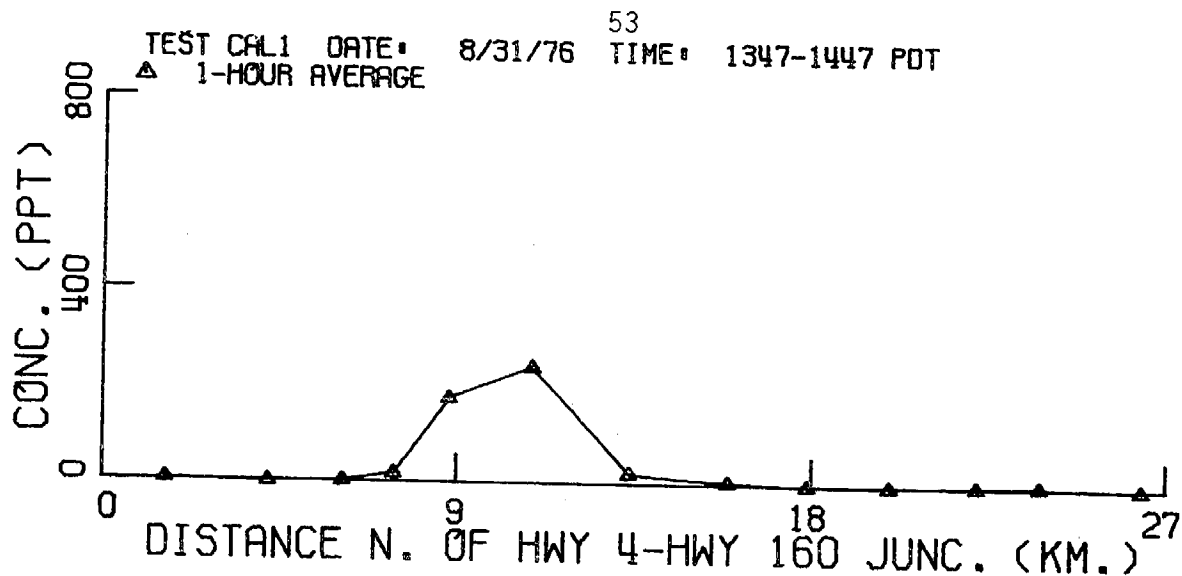


Figure 11. Hourly averaged crosswind  $SF_6$  profiles measured along Highway 160.

hourly plume was 72 km wide and was centered approximately 10 km north of Stockton. Significant levels of  $\text{SF}_6$  were detected during three hours along Highway 99. The tracer emitted during a five-hour period took only three hours to pass, implicating the existence of somewhat stagnant conditions downwind of the Montezuma Hills earlier in the afternoon. The hourly averaged concentrations are plotted as a function of the distance south of Sacramento in Figure 12. An overview of the hourly averaged results is provided in Figure 13.

#### 4.22 Tracer Test 2 (9/2/76)

The purpose of Test 2 was to tag the air moving over the Montezuma Hills during the afternoon Sea Breeze period. Two atmospheric tracers were used:  $\text{SF}_6$  was introduced upstream at Martinez near existing industrial pollutant sources;  $\text{CBrF}_3$  was released from the Montezuma Hills.  $\text{SF}_6$  was released at a steady rate of 11.4 g/sec (1.08 tons/day) from 1100 to 1600 PDT. The release of  $\text{CBrF}_3$  was not started until 1300 PDT in hopes of waiting for the  $\text{SF}_6$ -tagged air to reach the Montezuma Hills. The  $\text{CBrF}_3$  was released at a constant rate of 16.6 g/sec (1.58 tons/day) until 1500 PDT.

The average surface wind vectors at Martinez and at the Dow site were  $270^\circ$  at 4.0 m/sec and  $270^\circ$  at 9.2 m/sec, respectively. The overall area average wind direction and speed for the release period was  $290^\circ$  at 4.3 m/sec. The horizontal standard deviation of the winds at the Dow site was  $7^\circ$  for the day. The average mixing height in the area was 830 meters with a maximum of 1500 meters occurring during the late afternoon. There were no clouds, and Pasquill stability classes B-C were assumed to exist. The wind pattern at 1600 PDT shown in Figure 14 was typical for

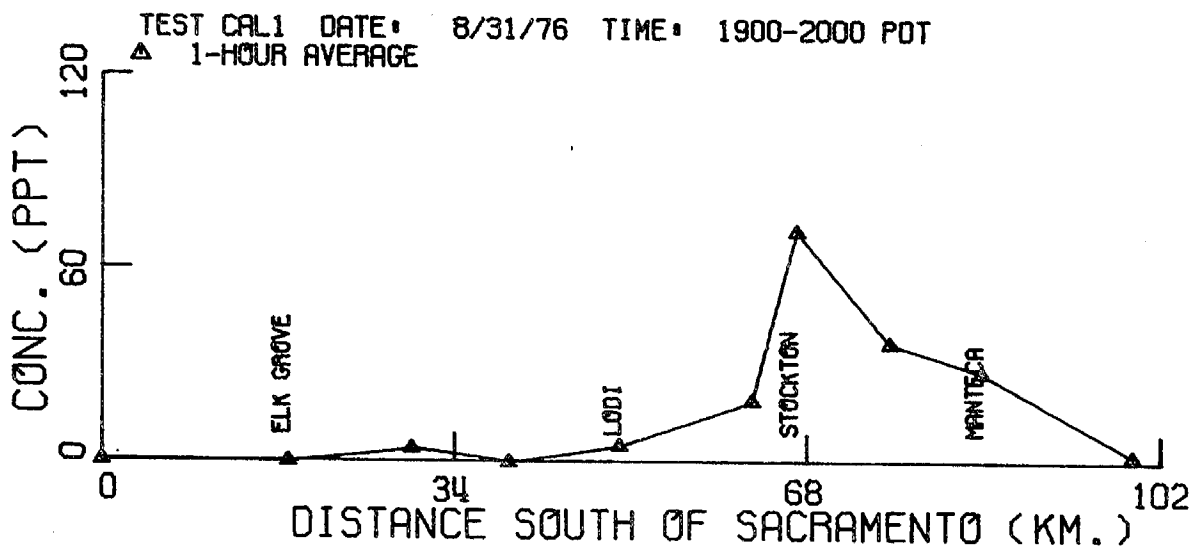
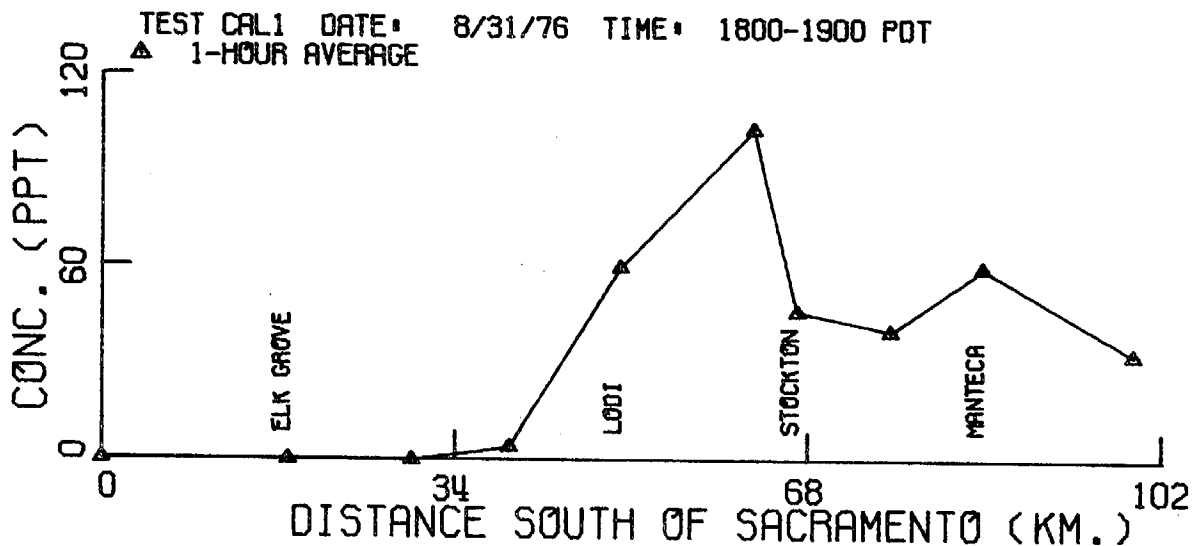
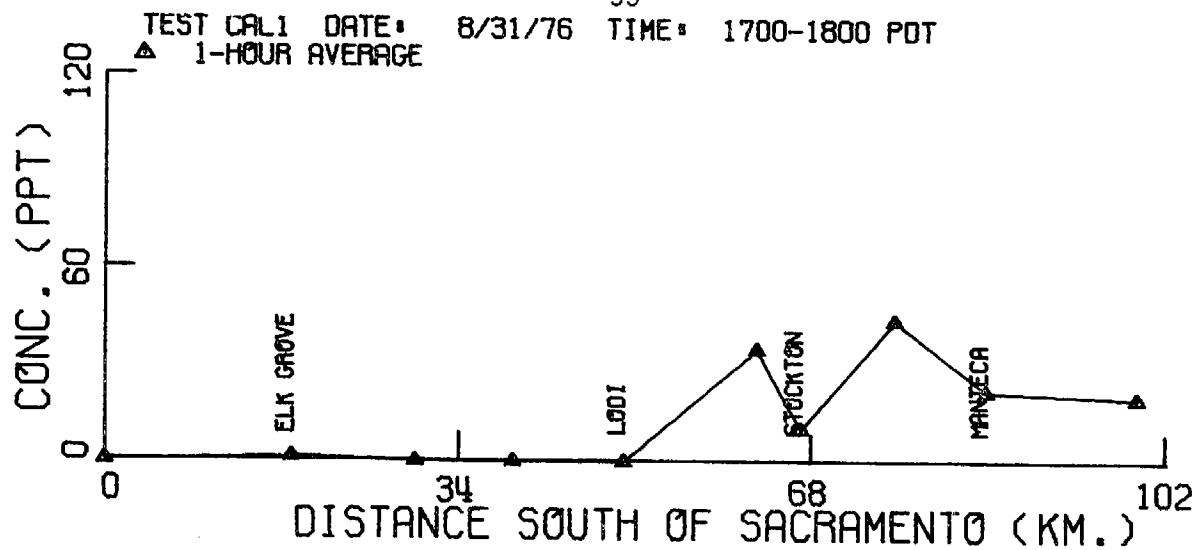


Figure 12. Hourly averaged crosswind  $SF_6$  profiles measured along Highway 99.

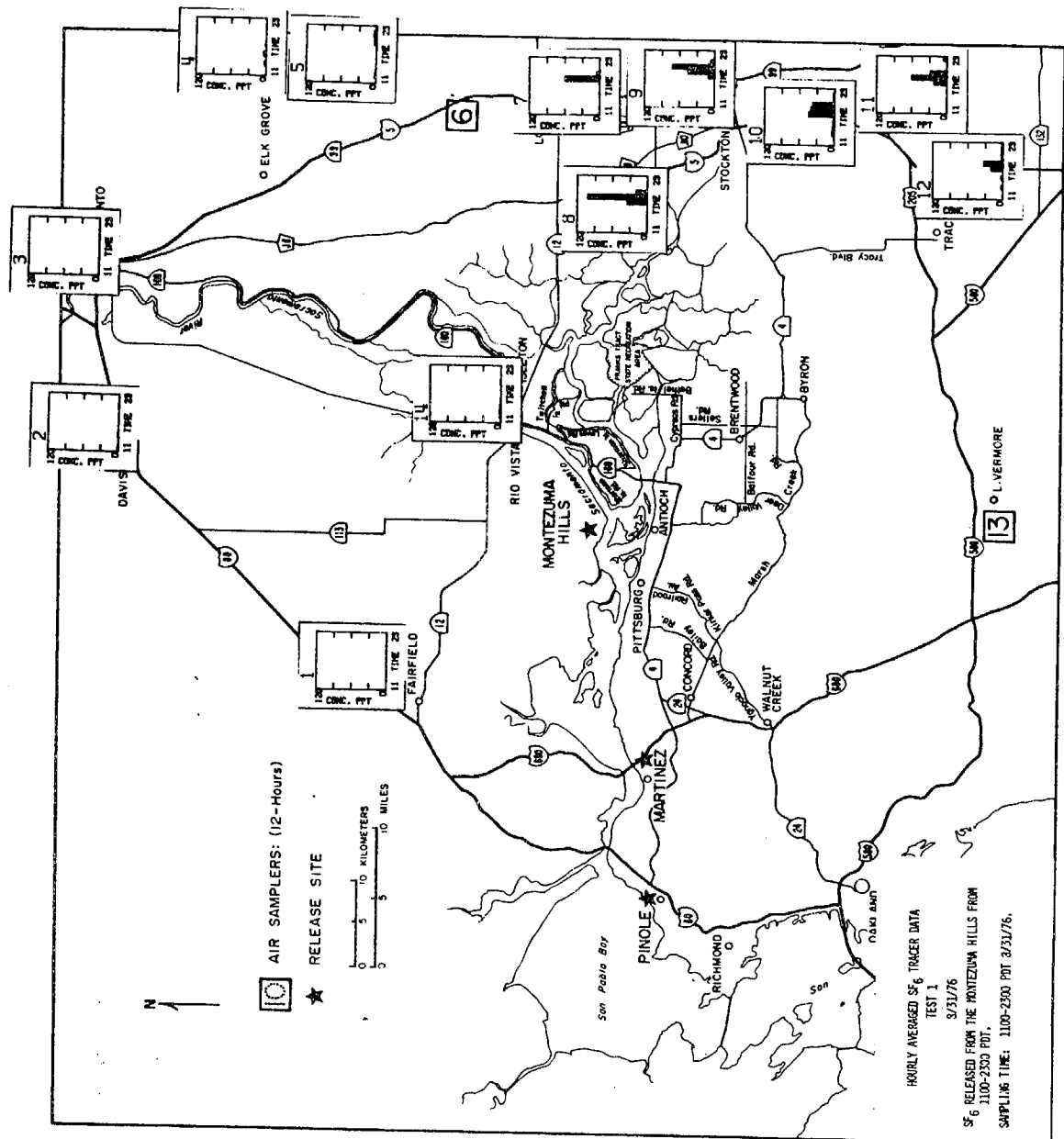


Figure 13. Overview of hourly averaged  $SF_6$  data. Full-scale  $SF_6 = 120$  ppt.

Figure 14. Surface wind streamlines, 1600 PDT, 9/2/76 (MRI).



the afternoon. The pattern appears to be similar to Smalley wind flow type W-6 which occurred 10% of the time in September and 6% of the time on a yearly basis between 1952 and 1955. The peak ozone level was 0.16 ppm observed at Stockton.

Eleven automobile traverses were conducted. The majority of the air tagged by the  $\text{SF}_6$  tracer did not pass over the Montezuma Hills. However, it did pass through the same downwind zone (i.e., the Tracy-Stockton area) as did the emissions from Montezuma Hills. Traverses 2 and 3 in Figure 15, Traverse 4 in Figure 16, and Traverse 10 in Figure 17 show the sharp, spiked  $\text{SF}_6$  and  $\text{CBrF}_3$  plumes immediately downwind of Martinez and Montezuma Hills, respectively, the broad  $\text{SF}_6$  plume crossing Highway 160, and the location of both tracer plumes crossing Highway 99 south of Stockton. The maximum  $\text{SF}_6$  concentration observed along Highway 160, 35 km downwind of Martinez, was 33 ppt, while the maximum level seen along Highway 99, 67 km downwind, was 91 ppt. The profile in Traverse 3 indicates that the  $\text{SF}_6$  trajectory passed south of the Montezuma Hills below Pittsburg and Antioch. The  $\text{SF}_6$  profile in Traverse 10 suggests that a portion of the tracer from Martinez moved south through the Walnut Creek area towards Livermore.

The  $\text{CBrF}_3$  plume behaved in a manner similar to that observed during Test 1. The plume crossed Highway 160 approximately 8.2 km north of the Highway 160-Highway 4 junction with a peak concentration of 2168 ppt. It appeared to curve south toward Stockton, crossing Highway 99 with a peak concentration of 300 ppt, 57 km downwind.

Hourly averaged data obtained along Highway 160 and shown in Figure 18 confirm the description drawn from the traverse data. The

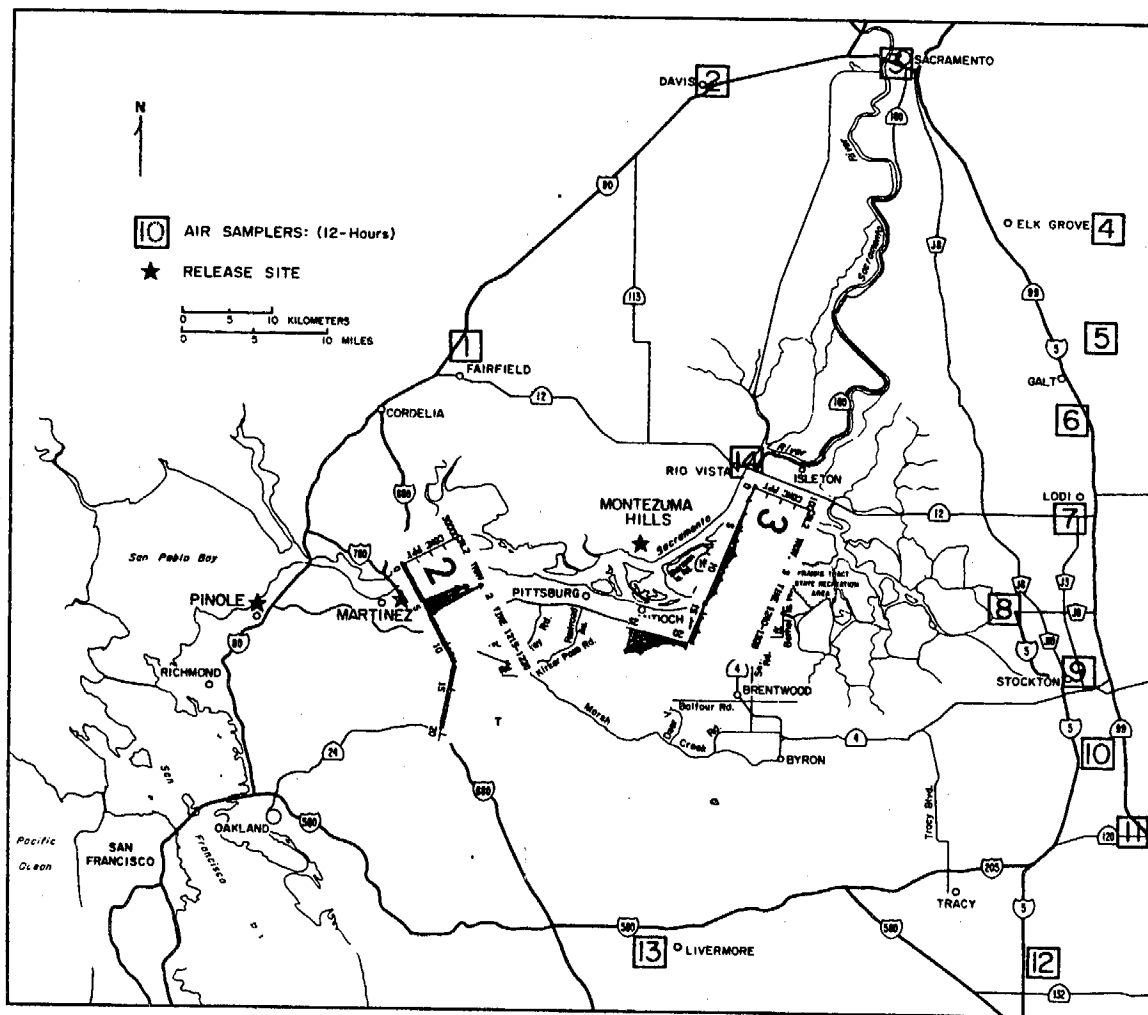


Figure 15. Overview of automobile traverse SF<sub>6</sub> data.

## TEST 2

9/2/76

### Auto Traverses:

2 1215 - 1228 PDT, SF<sub>6</sub>(max) = 30,000 ppt

3 1240 - 1328 PDT, SF<sub>6</sub>(max) - 41 ppt

SF<sub>6</sub> released from Martinez from 1100-1600 PDT.

CBrF<sub>3</sub> released from the Montezuma Hills from 1300-1500 PDT.



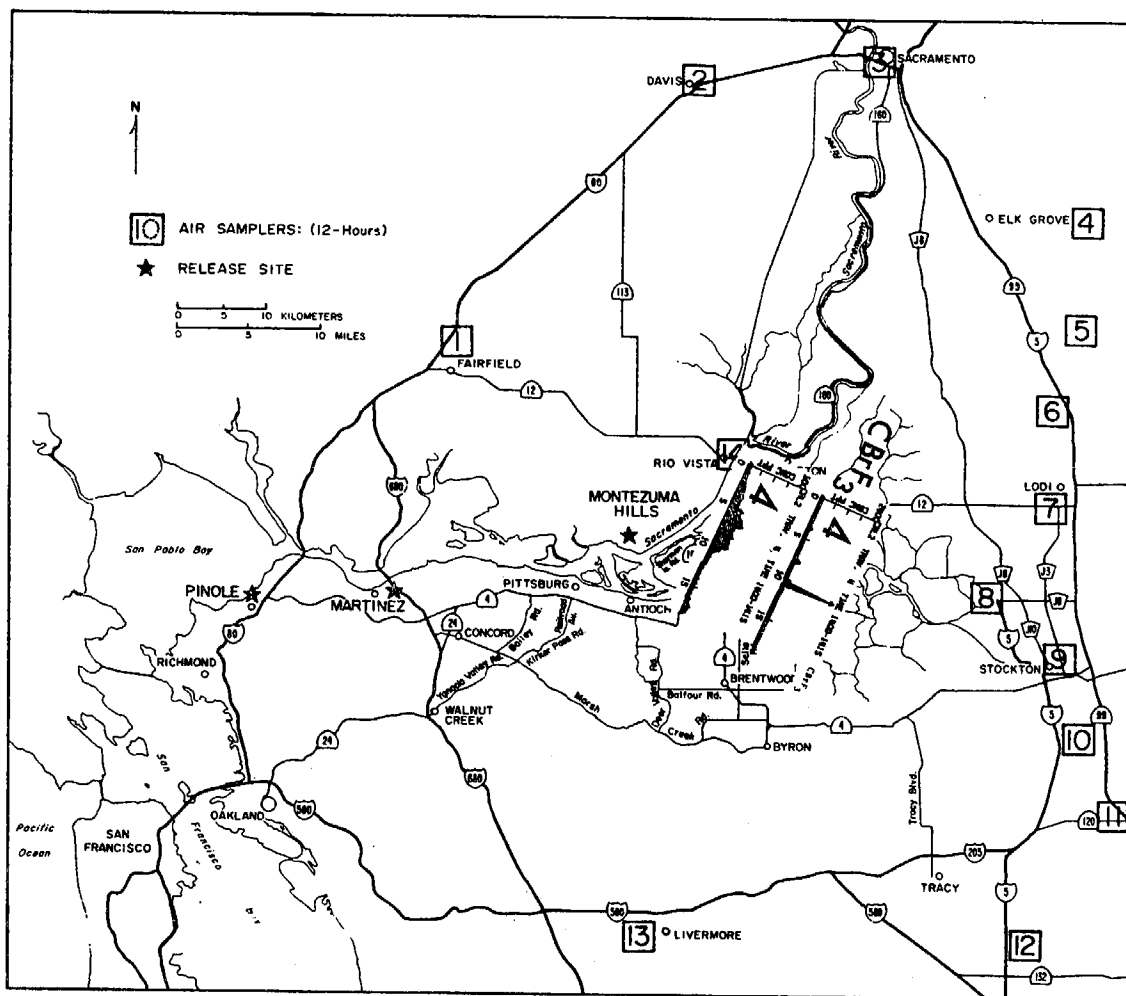


Figure 16. Overview of automobile traverse SF<sub>6</sub> and CBrF<sub>3</sub> data.

TEST 2

9/2/76

**Auto Traverse:**

4 1400-1415 PDT, SF<sub>6</sub>(max) = 33 ppt.

1400-1415 PDT, CBrF<sub>3</sub>(max) = 2168 ppt.

SF<sub>6</sub> released from Martinez from 1100-1600 PDT.

CBrF<sub>3</sub> released from the Montezuma Hills from 1300-1500 PDT.

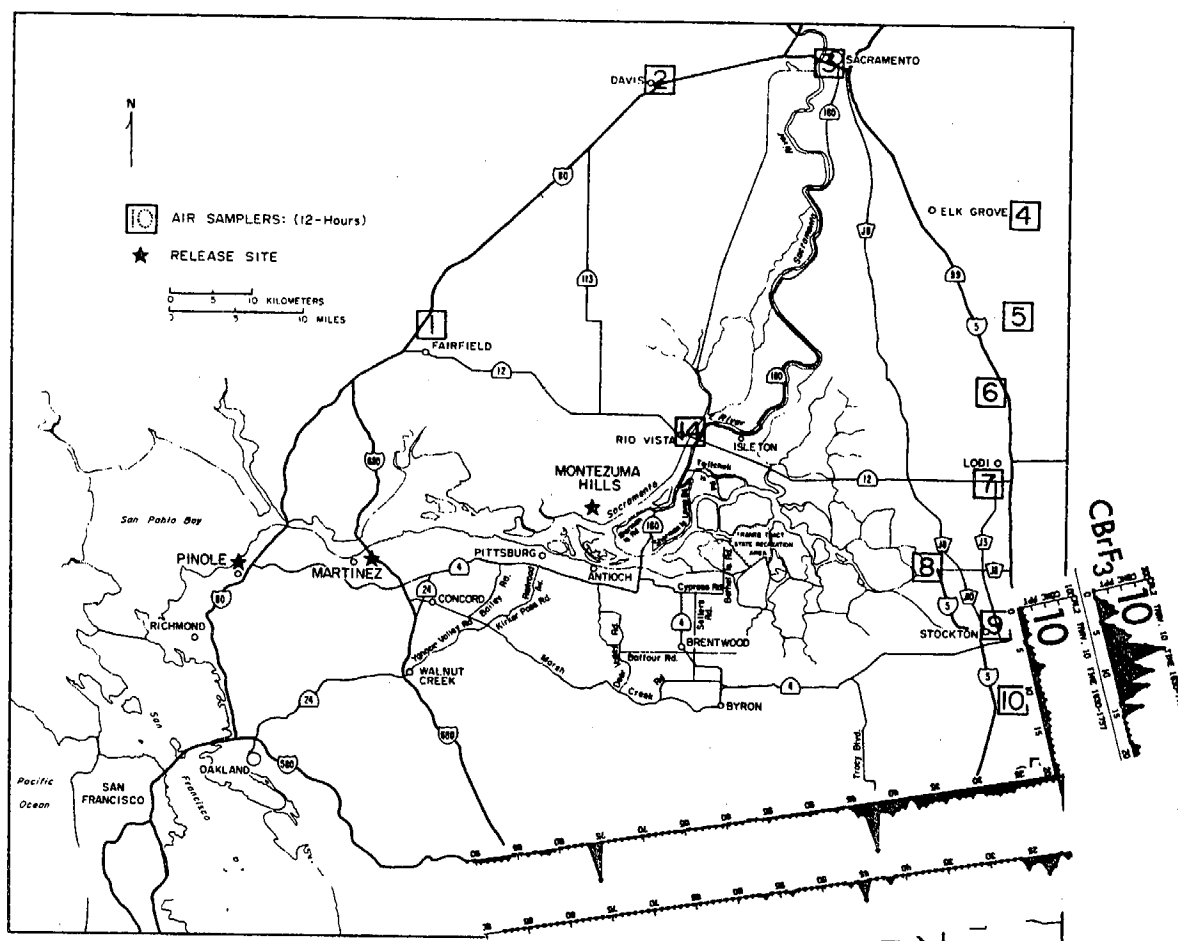


Figure 17. Overview of automobile traverse  $\text{SF}_6$  and  $\text{CBrF}_3$  data.

TEST 2

9/2/76

Auto Traverse:

10 1630-1737 PDT,  $\text{SF}_6(\text{max}) = 91$  ppt.

1630-1737 PDT,  $\text{CBrF}_3(\text{max}) = 300$  ppt.

$\text{SF}_6$  released from Martinez from 1100-1600 PDT.

$\text{CBrF}_3$  released from the Montezuma Hills from 1300-1500 PDT.

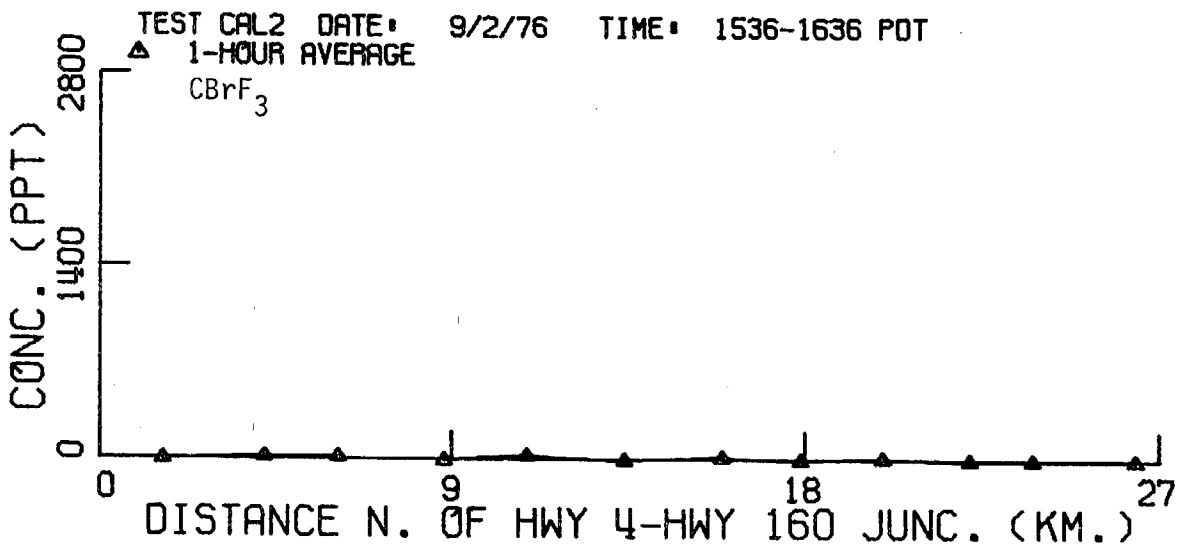
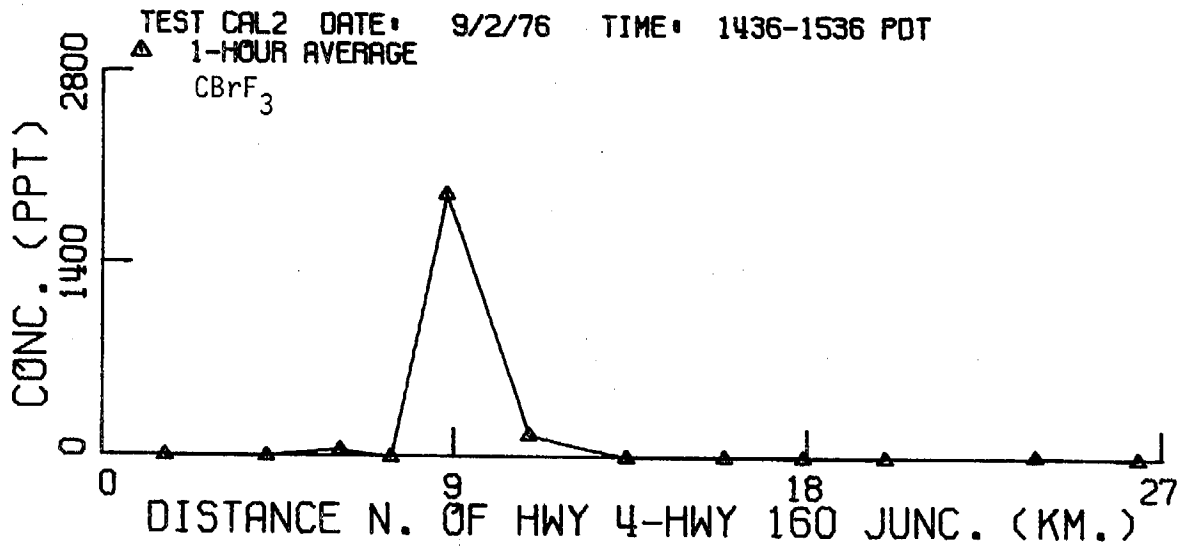
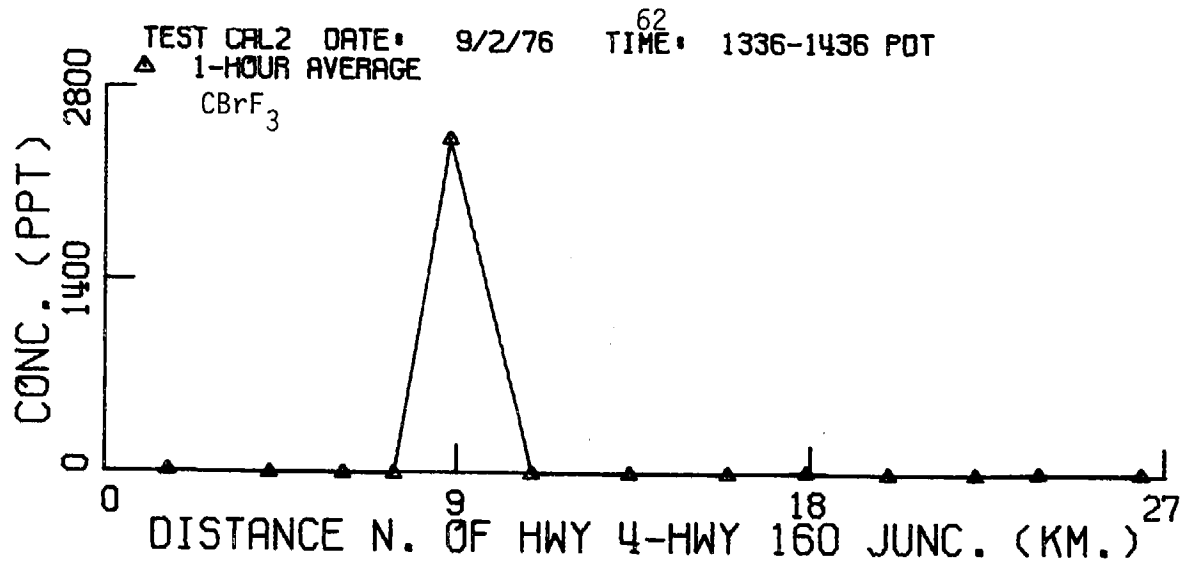


Figure 18. Hourly averaged crosswind CBrF<sub>3</sub> profiles measured along Highway 160.

SF<sub>6</sub> profile stretches along Highway 160 for 26 km with a maximum of 17 ppt as shown in Figure 19. The maximum hourly averaged concentration of CBrF<sub>3</sub> along Highway 160 was 2427 ppt observed 8.8 km north of the Highway 160-Highway 4 junction. The overview map in Figure 20 shows the widespread detection of SF<sub>6</sub> during the test period. The data shown in Figure 21 indicate that the plume reached Stockton at about 1600 PDT, which corresponds to an average transport wind speed of 4 m/sec (14 km/hr). The maximum SF<sub>6</sub> concentration along Highway 99 was 21 ppt observed approximately 9 km south of Stockton at 1800 PDT. In this test, measurable levels of SF<sub>6</sub> were obtained during the night and early morning at several stations along Highway 99. These levels were less than 10 ppt; they suggest that possibly the tracer emitted near the end of the release period from Martinez was transported into the Stockton-Tracy area where it remained for several hours under nighttime stagnant conditions. As in the first test, material emitted from the Montezuma Hills reached the Stockton area and was directed south into the San Joaquin Valley. In addition, material emitted from Martinez, near the Carquinez Strait, reached the same area and appeared to be moving south into the San Joaquin Valley.

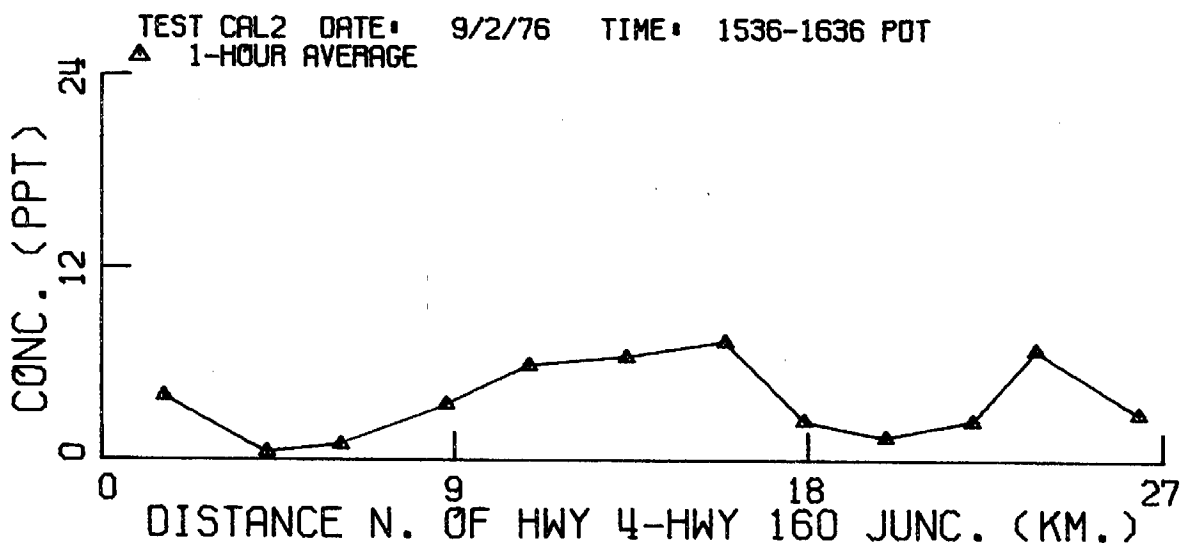
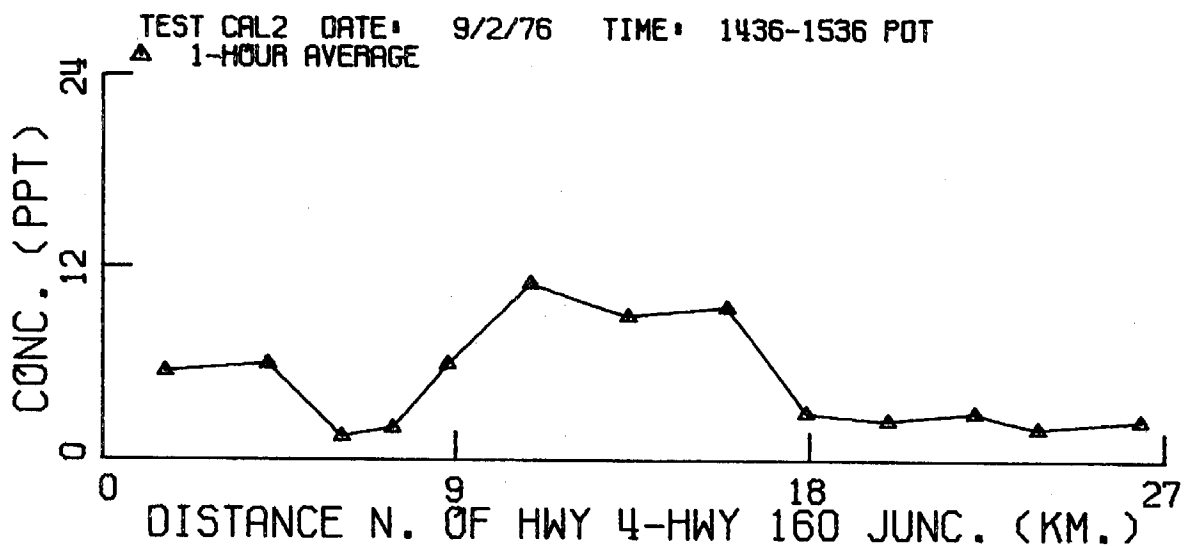
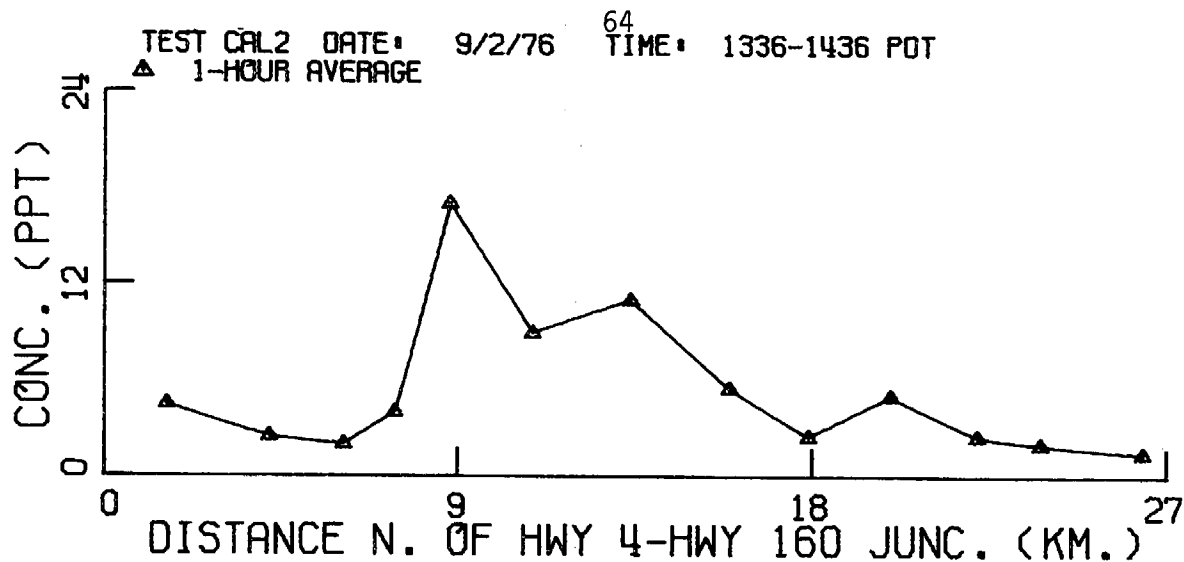


Figure 19. Hourly averaged crosswind  $SF_6$  profiles measured along Highway 160.

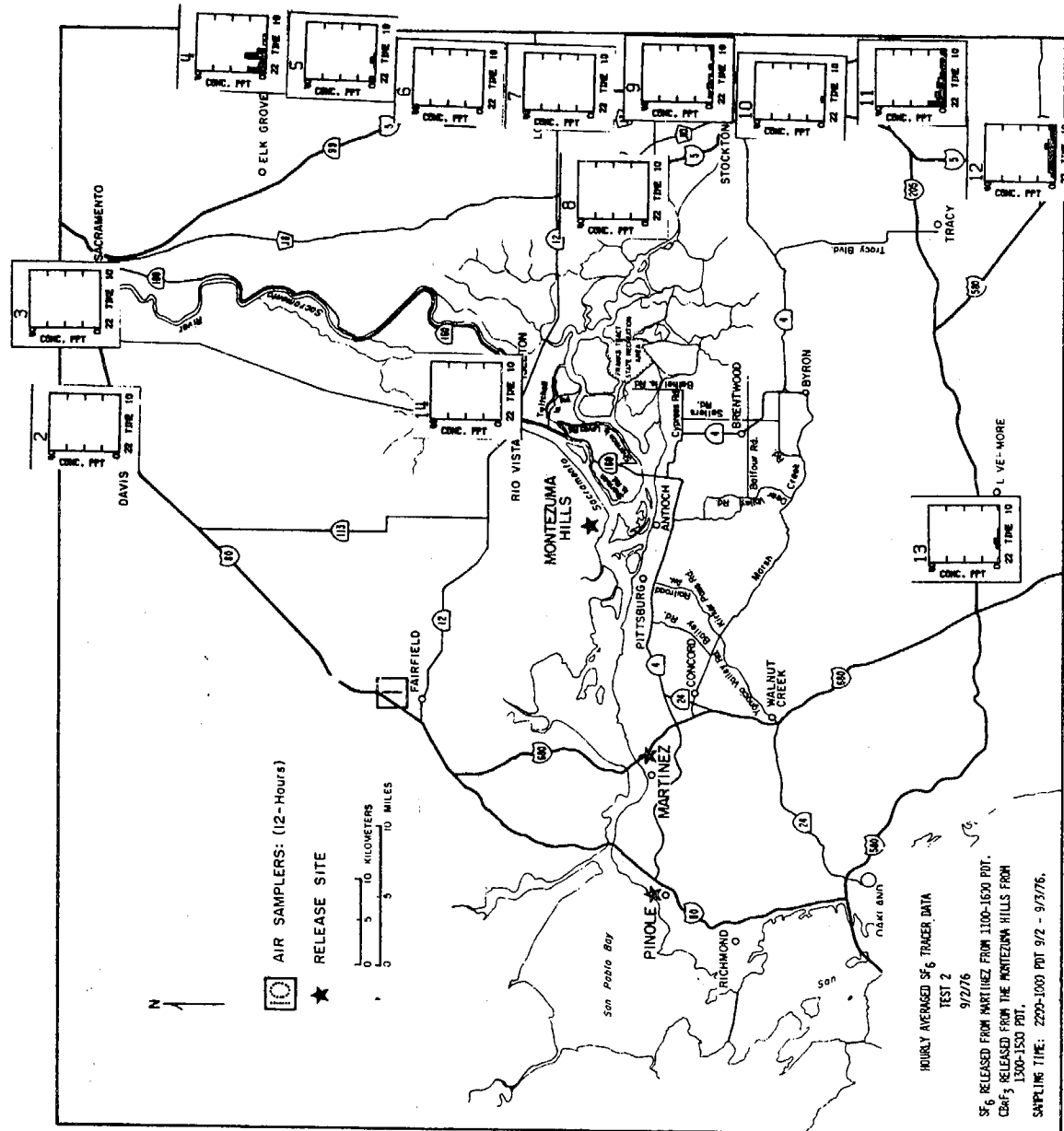


Figure 20. Overview of hourly averaged  $SF_6$  data. Full scale  $SF_6 = 40$  ppt.

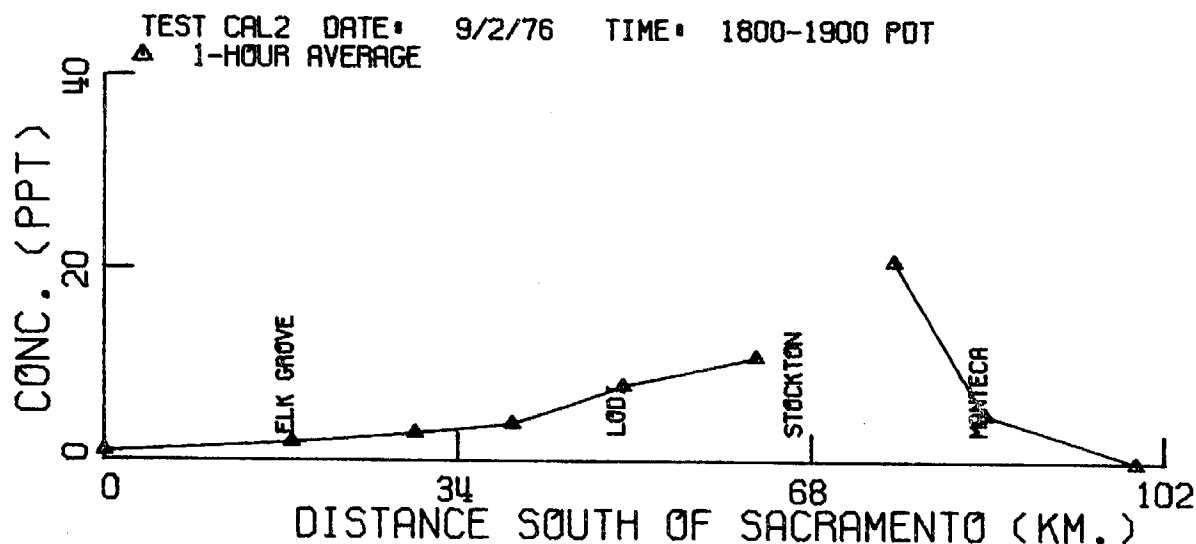
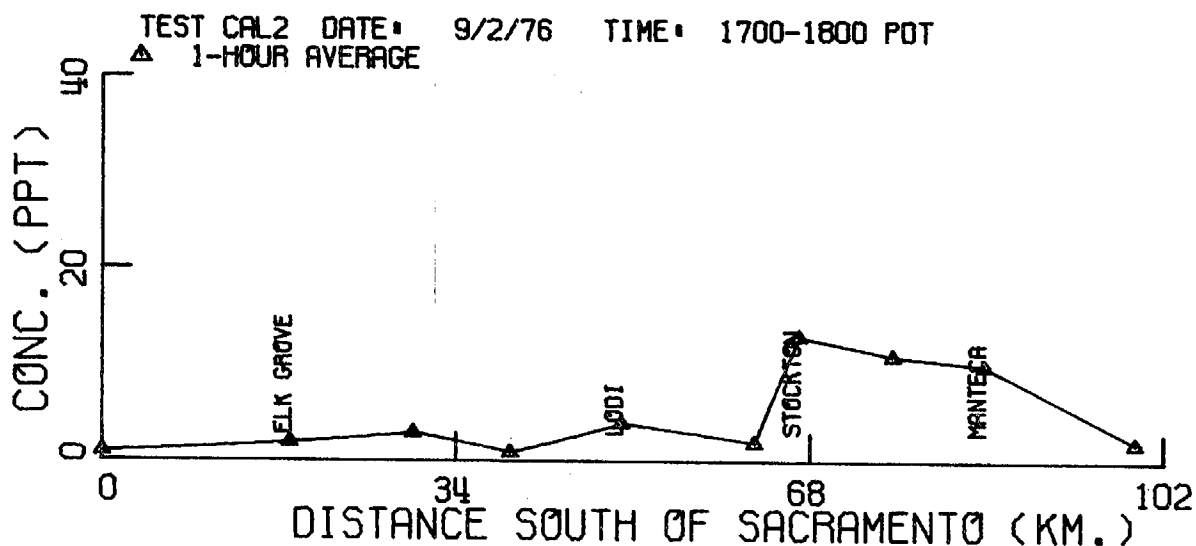
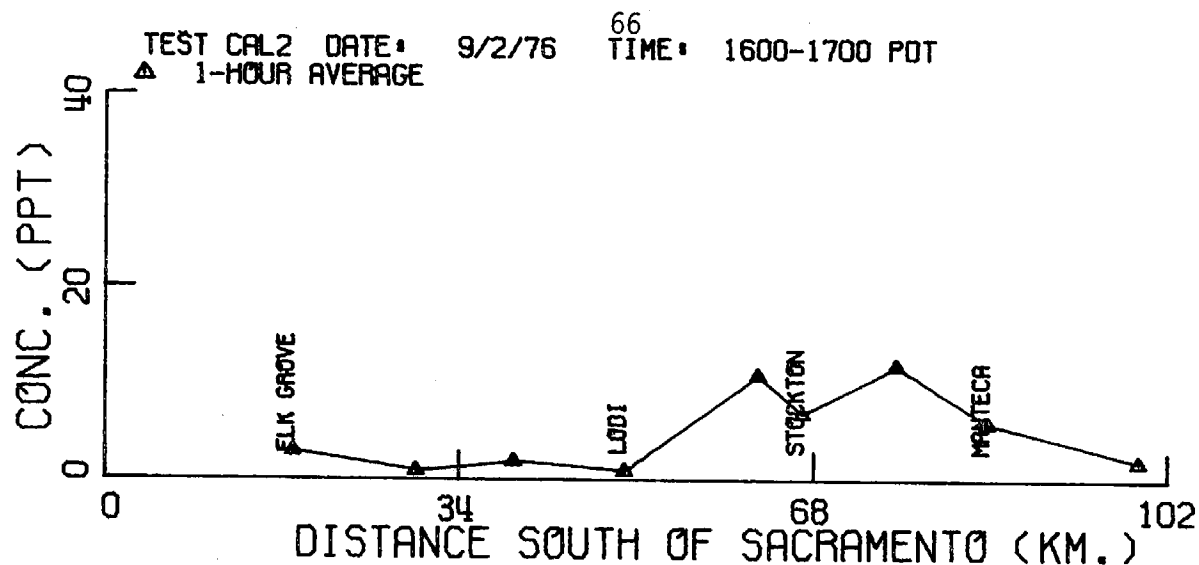


Figure 21. Hourly averaged  $SF_6$  profiles measured along Highway 99.